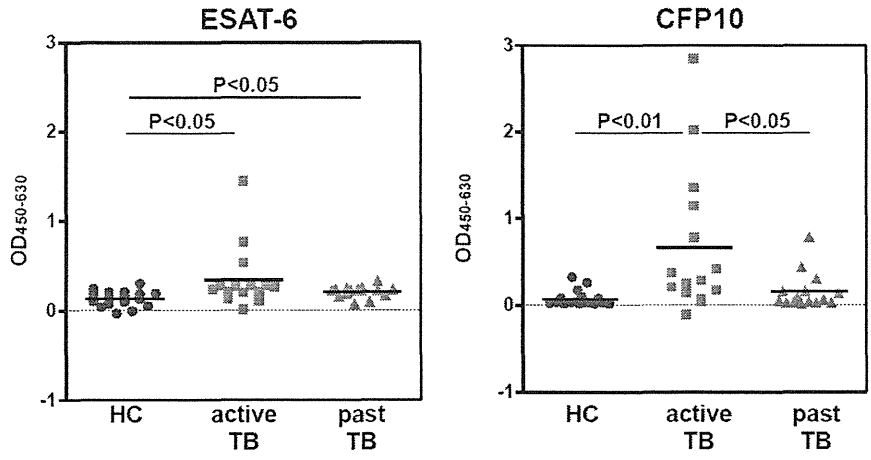
ESAT-6
CFP10
P<0.05
P<0.05
P<0.01
P<0.05
OD450-630
3
2
1
0
-1
HC
active TB
past TB

Figure. 1

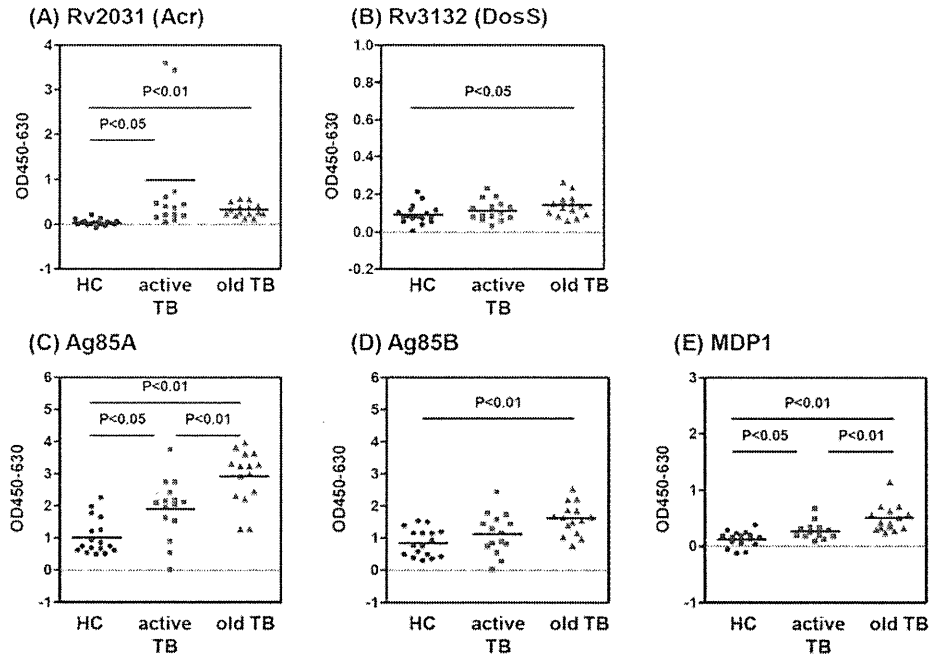
(A) Rv2031 (Acr)
(B) Rv3132 (DosS)
(C) Ag85A
(D) Ag85B
(E) MDP1
OD450-630
P<0.01
P<0.05
HC
active TB
old TB

Figure. 2

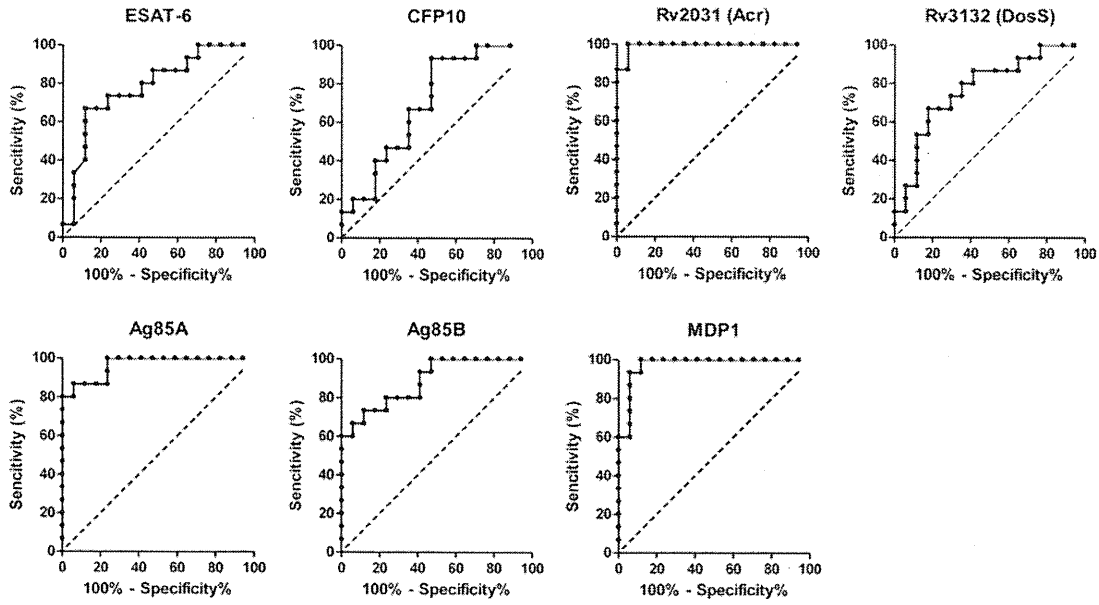
ESAT-6
CFP10
Rv2031 (Acr)
Rv3132 (DosS)
Ag85A
Ag85B
MDP1
Sencitivity (%)
100% - Specificity%
0
20
40
60
80
100

Figure. 3

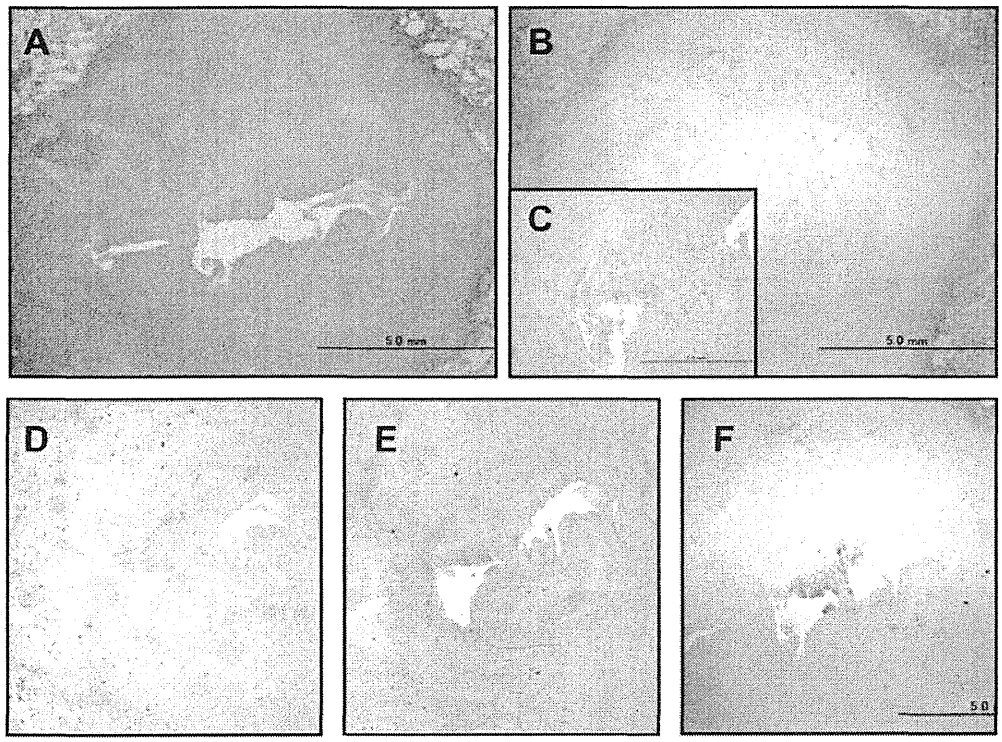

Figure. 4

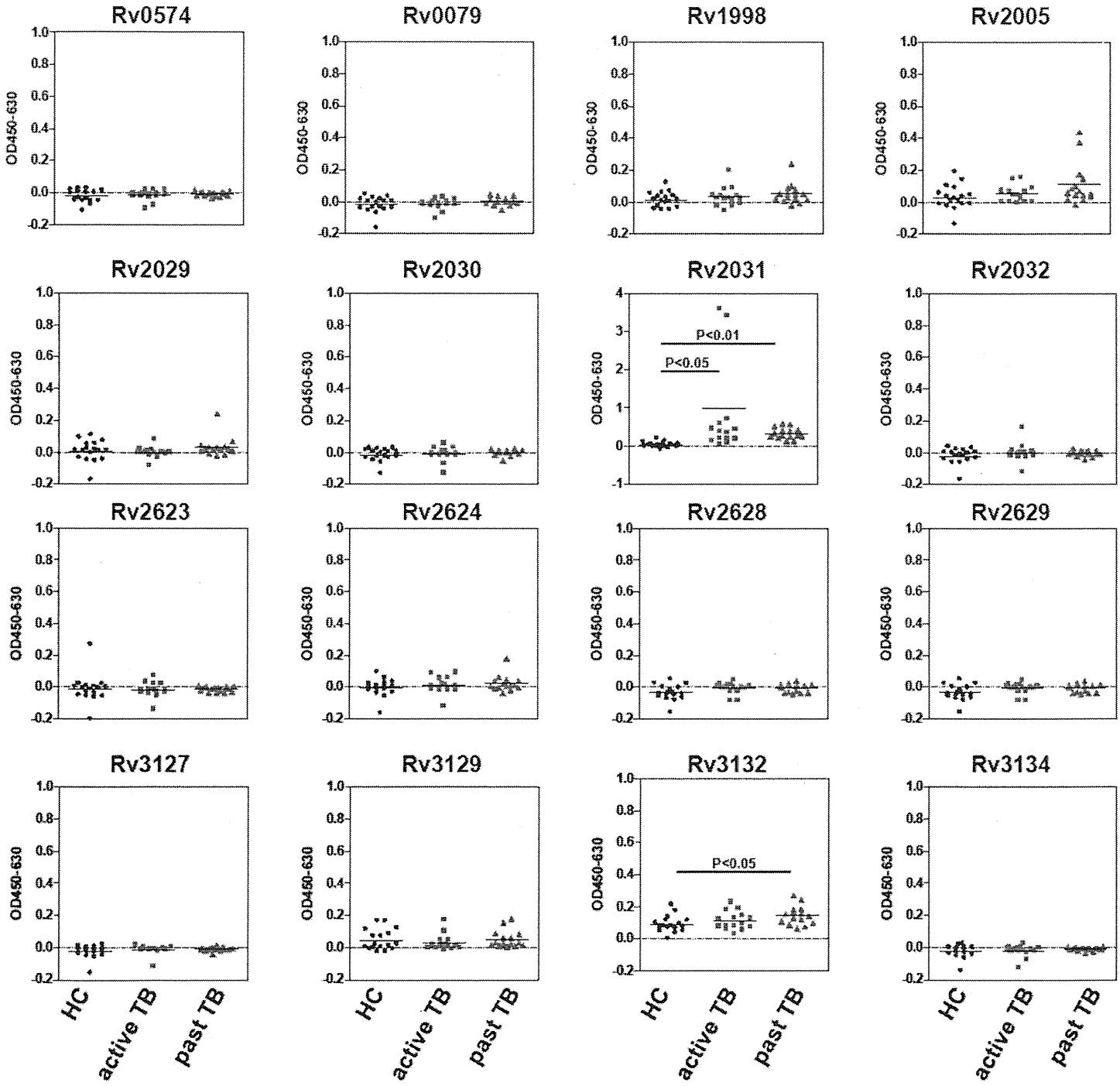
Rv0574
Rv0079
Rv1998
Rv2005
Rv2029
Rv2030
Rv2031
Rv2032
Rv2623
Rv2624
Rv2628
Rv2629
Rv3127
Rv3129
Rv3132
Rv3134
OD450-630
P<0.01
P<0.05
HC
active TB
past TB

JB Journals.ASM.org

GENOME ANNOUNCEMENT

Whole-Genome Sequence of the Hypervirulent Clinical Strain *Mycobacterium intracellulare* M.i.198

Yoshitaka Tateishi,[a,b] Seigo Kitada,[b] Keisuke Miki,[b] Ryoji Maekura,[b] Yoshitoshi Ogura,[c] Yuriko Ozeki,[a] Yukiko Nishiuchi,[a] Mamiko Niki,[a] Tetsuya Hayashi,[c] Kazuto Hirata,[d] Kazuo Kobayashi,[e] and Sohkichi Matsumoto[a]

Department of Bacteriology, Graduate School of Medicine, Osaka City University, Osaka, Japan[a]; National Hospital Organization, Toneyama Hospital, Osaka, Japan[b]; Department of Life Science, Frontier Science Research Center, University of Miyazaki, Miyazaki, Japan[c]; Department of Respiratory Medicine, Graduate School of Medicine, Osaka City University, Osaka, Japan[d]; and Department of Immunology, National Institute of Infectious Diseases, Tokyo, Japan[e]

We report herein the draft genome sequence of *Mycobacterium intracellulare* clinical strain M.i.198, which consistently exhibits hypervirulence in human patients, human macrophages *in vitro*, and immunocompetent mice.

Nontuberculous mycobacteria are of great clinical importance with respect to the recent increasing prevalence of nontuberculous mycobacterioses, such as *Mycobacterium avium* complex (MAC) disease, which is difficult to treat without specific antibiotics (1). However, the bacteriological etiology of nontuberculous mycobacteria remains to be elucidated. We identified a hypervirulent *Mycobacterium intracellulare* strain (M.i.198) from an immunocompetent patient with pulmonary MAC disease (5). To help understand the genetic background of the virulence, we performed whole-genome sequencing of strain M.i.198.

We sequenced *M. intracellulare* M.i.198 genomic DNA on a Roche 454 FLX Titanium sequencer and assembled the reads using the software program Newbler v2.3. A total of 924,616 reads was generated, with an average read length of 246 bp, yielding a total sequence of 227,524,944 bp.

The assembled sequences contained 149 contigs, and the length of all contigs combined was 5,406,664 bp, with a G+C ratio of 68.0%. The average coverage depth was 42.1×, the N_{50} contig size was 90,025 bp, the average contig was 40,008 bp long, and the longest contig was 453,296 bp. The final assembly comprised 122 contigs in five scaffolds (99.7% of contig bases). We constructed an optical map (OpGen) of strain M.i.198 with the NheI restriction enzyme, yielding 311 ordered restriction fragments (average fragment size, 16 kb). The genome size was estimated to be approximately 5.22 Mb; this was obtained from the sum of all restriction fragments. The five scaffolds were placed on the map, confirming a single circular chromosome without plasmids.

Genome annotation using the NCBI Prokaryotic Genomes Automatic Annotation Pipeline (http://www.ncbi.nlm.nih.gov/genomes/static/Pipeline.html) identified 5,146 coding sequences (CDSs). Strain M.i.198 has three rRNAs (in a single rRNA operon) and 48 tRNA genes.

We compared the sequence of M.i.198 with those of three other recently sequenced *M. intracellulare* strains: ATCC 13950 (GenBank accession no. CP003322.1), MOTT-02 (GenBank accession no. CP003323.1), and MOTT-64 (GenBank accession no. CP003324.1)—the latter two were clinical isolates from Korean patients (2, 3, 4). The reciprocal best-hit BLAST approach revealed that strain M.i.198 shares 90.0%, 92.7%, and 88.7% of its CDSs with *M. intracellulare* ATCC 13950, MOTT-02, and MOTT-64, respectively. Of particular interest is a 51-kb region of difference, 55 CDSs in length (G+C ratio, 61.0%), which consists of prophages in M.i.198. The genome sequence of strain M.i.198 will provide an invaluable resource for understanding the microbiological aspects of human-pathogen interactions, especially the pathogenesis of human MAC disease.

Nucleotide sequence accession numbers. The whole-genome sequence of M.i.198 has been deposited in DDBJ/EMBL/GenBank under the accession numbers BAGQ01000001 to BAGQ01000149.

ACKNOWLEDGMENTS

This work was funded by grants from the Ministry of Education, Culture, Sports, Science and Technology of Japan, the Ministry of Health, Labor, and Welfare (Research on Emerging and Reemerging Infectious Diseases, Health Sciences Research Grants) of Japan, the Japan Health Sciences Foundation, and the United States-Japan Cooperative Medical Science Program against Tuberculosis and Leprosy.

REFERENCES

1. **Griffith DE, et al.** 2007. An official ATS/IDSA statement: diagnosis, treatment, and prevention of nontuberculous mycobacterial diseases. Am. J. Respir. Crit. Care Med. 175:367–416.
2. **Kim BJ, Choi BS, Lim JS, Choi IY, Kook YH.** 2012. Complete genome sequence of *Mycobacterium intracellulare* clinical strain MOTT-64, belonging to the INT1 genotype. J. Bacteriol. **194**:3268.
3. **Kim BJ, et al.** 2012. Complete genome sequence of *Mycobacterium intracellulare* clinical strain MOTT-02. J. Bacteriol. **194**:2771.
4. **Kim BJ, et al.** 2012. Complete genome sequence of *Mycobacterium intracellulare* strain ATCC 13950^T. J. Bacteriol. **194**:2750.
5. **Tateishi Y, et al.** 2009. Virulence of *Mycobacterium avium* complex strains isolated from immunocompetent patients. Microb. Pathog. **46**:6–12.

Received 10 August 2012 **Accepted** 10 September 2012

Address correspondence to Yoshitaka Tateishi, y-tateishi@med.osaka-cu.ac.jp, or Sohkichi Matsumoto, sohkichi@med.osaka-cu.ac.jp.

Y.T. and S.M. contributed equally to this article.

doi:10.1128/JB.01439-12

THE JOURNAL OF BIOLOGICAL CHEMISTRY VOL. 287, NO. 33, pp. 27743–27752, August 10, 2012

A Novel Mechanism of Growth Phase-dependent Tolerance to Isoniazid in Mycobacteria*

Received for publication, December 13, 2011, and in revised form, May 27, 2012 Published, JBC Papers in Press, May 30, 2012, DOI 10.1074/jbc.M111.333385

Makoto Niki[‡], Mamiko Niki[‡1], Yoshitaka Tateishi[‡§], Yuriko Ozeki[‡¶], Teruo Kirikae[‖], Astrid Lewin[**], Yusuke Inoue[‡‡], Makoto Matsumoto[‡‡], John L. Dahl[§§], Hisashi Ogura[¶¶], Kazuo Kobayashi[‖‖], and Sohkichi Matsumoto[‡2]

*From the [‡]Departments of Bacteriology and [¶¶]Virology, Osaka City University Graduate School of Medicine, 1-4-3 Asahi-machi, Abeno-ku, Osaka 545-8585, Japan, the [§]Department of Internal Medicine, National Hospital Organization Toneyama National Hospital, 5-1-1 Toneyama, Toyonaka, Osaka 560-8552, Japan, the [¶]Department of Food and Nutrition, Sonoda Women's University, 7-29-1 Minamitsukaguchi-cho, Amagasaki, Hyogo 661-8520, Japan, the [‖]National Center for Global Health and Medicine, 1-21-1 Toyama, Shinjuku, Tokyo 162-8655, Japan, the **Robert Koch Institute, Nordufer 20, 13353 Berlin, Germany, the [‡‡]Microbiological Research Institute, Otsuka Pharmaceutical, Kagasuno, Kawauchi-cho, Tokushima 771-0192, Japan, the [§§]Department of Biology, University of Minnesota Duluth, Duluth, Minnesota 55812, and the [‖‖]Department of Immunology, National Institute of Infectious Diseases, 1-23-1 Toyama, Shinjuku-ku, Tokyo 162-8640, Japan*

Background: The mechanism underlying mycobacterial phenotypic tolerance to isoniazid is unknown.
Results: MDP1, a mycobacterial histone-like protein, down-regulates KatG expression.
Conclusion: Down-regulation of KatG by MDP1 causes growth phase-dependent phenotypic tolerance to isoniazid in mycobacteria.
Significance: Understanding the mechanism by which mycobacteria acquire tolerance to isoniazid is important for developing novel therapies.

Tuberculosis remains one of the most deadly infectious diseases worldwide and is a leading public health problem. Although isoniazid (INH) is a key drug for the treatment of tuberculosis, tolerance to INH necessitates prolonged treatment, which is a concern for effective tuberculosis chemotherapy. INH is a prodrug that is activated by the mycobacterial enzyme, KatG. Here, we show that mycobacterial DNA-binding protein 1 (MDP1), which is a histone-like protein conserved in mycobacteria, negatively regulates *katG* transcription and leads to phenotypic tolerance to INH in mycobacteria. *Mycobacterium smegmatis* deficient for MDP1 exhibited increased expression of KatG and showed enhanced INH activation compared with the wild-type strain. Expression of MDP1 was increased in the stationary phase and conferred growth phase-dependent tolerance to INH in *M. smegmatis*. Regulation of KatG expression is conserved between *M. smegmatis* and *Mycobacterium tuberculosis* complex. Artificial reduction of MDP1 in *Mycobacterium bovis* BCG was shown to lead to increased KatG expression and susceptibility to INH. These data suggest a mechanism by which phenotypic tolerance to INH is acquired in mycobacteria.

Tuberculosis is a disease caused by infection with *Mycobacterium tuberculosis* complex and remains a serious threat to health around the world. Approximately one-third of the world's population is infected with *M. tuberculosis*. The current World Health Organization report shows that 8.8 million new tuberculosis cases arose, and 1.4 million people died from tuberculosis in 2010. Although medications are indispensable for treating infectious diseases, one of the predominant problems in tuberculosis chemotherapy is the prolonged treatment duration. The current treatment of tuberculosis with first-line antitubercular agents including isoniazid (isonicotinic acid hydrazide, INH)[3], rifampin, pyrazinamide, streptomycin, and ethambutol requires at least six months to cure the acute disease, yet there is still a relapse rate of 2 to 3% (1). For latent tuberculosis, the standard treatment takes six to nine months using INH alone.

The relatively long duration of tuberculosis chemotherapy is not only due to reduced metabolism based on the slow growth rates of the pathogens but also the emergence of drug-resistant cells. There are two possible mechanisms by which *M. tuberculosis* acquires drug resistance. First, spontaneous chromosomal mutations in genes related to drug resistance can result from irregular drug supply, inappropriate drug prescriptions, and poor patient adherence to treatment (2). Secondly, *M. tuberculosis* can acquire phenotypic drug resistance in the absence of genotypic alterations in drug-target genes (3). In particular, it is well known that INH tolerance is acquired by *M. tuberculosis*

* This work was supported by grants from the Ministry of Education, Culture, Sports, Science, and Technology, the Ministry of Health, Labor, and Welfare (Research on Emerging and Re-emerging Infectious Diseases, Health Sciences Research Grants), The Japan Health Sciences Foundation, and The United States-Japan Cooperative Medical Science Program against Tuberculosis and Leprosy.

[1] To whom correspondence may be addressed: Dept. of Bacteriology, Osaka City University Graduate School of Medicine, 1-4-3 Asahi-machi, Abeno-ku, Osaka 545-8585, Japan. Tel.: 81-6-6645-3745; Fax: 81-6-6645-3746; E-mail: myoshi@med.osaka-cu.ac.jp.

[2] To whom correspondence may be addressed: Dept. of Bacteriology, Osaka City University Graduate School of Medicine, 1-4-3 Asahi-machi, Abeno-ku, Osaka 545-8585, Japan. Tel.: 81-6-6645-3745; Fax: 81-6-6645-3746; E-mail: sohkichi@med.osaka-cu.ac.jp.

[3] The abbreviations used are: INH, isoniazid; BCG, *Mycobacterium bovis* bacillus Calmette-Guérin; MDP1, mycobacterial DNA-binding protein 1; MIC, minimum inhibitory concentration; NBT, Nitroblue tetrazolium; ADC, albumin-dextrose-catalase; qRT-PCR, quantitative RT-PCR; ANOVA, analysis of variance.

during the stationary phase, and requires prolonged tuberculosis chemotherapy.

INH is one of the key drugs used to control tuberculosis (4). It is critical in tuberculosis therapy because of its potent bactericidal activity against organisms growing actively in the pulmonary cavities, whereas the sterilizing activity of INH is reduced nearly 1,000-fold in *M. tuberculosis* cells during the stationary phase of growth (5).

The mode of action of this drug is complicated. INH is a prodrug that is converted into the active form by the mycobacterial catalase-peroxidase, KatG (6). The expression of KatG is regulated by an iron-containing transcription factor, *furA*, which is situated immediately upstream of *katG* (7). In its active form, INH inhibits both InhA, which is a primary target of INH (8), and an enoyl-acyl carrier protein reductase of the fatty acid synthase II (9, 10).

DNA sequencing of INH-resistant clinical isolates has revealed several mutations associated with resistance to INH. In addition to mutations in *katG* and *inhA*, *ahpC* (coding for alkyl hydroperoxide) (11) and *ndh* (coding for NADH dehydrogenase) (12) have also been reported to be associated with INH resistance. Mutations in *kasA*, which encodes ketoacyl acyl carrier protein synthase, are involved in INH resistance (13). However, later studies showed that overexpression of KasA did not lead to INH resistance in *M. tuberculosis* (14), and mutations in *kasA* are not likely to participate in INH resistance (4). Among these mechanisms, INH resistance in *M. tuberculosis* is most commonly associated with mutations in *katG*. In addition, a recent study by Ando *et al.* (15) revealed that mutations in the intergenic region of *furA* and *katG* also affected *katG* expression and conferred INH resistance. Although the reason why mycobacteria in the stationary phase acquire INH tolerance has not been fully elucidated, it is likely that the regulated expression of genes involved in the action of this drug is responsible for INH tolerance.

Transcriptional regulators are thought to play important roles in growth phase-dependent bacterial adaptive responses, including drug tolerance. Histone-like proteins are possible candidate transcriptional regulators in such responses. Recently, it was reported that Lsr2, a histone-like protein highly conserved in mycobacteria, inhibits a wide variety of DNA-interacting enzymes to regulate genes induced by antibiotics and those associated with inducible multidrug tolerance (16). Mycobacterial DNA-binding protein 1 (MDP1) is another histone-like protein in mycobacteria that binds to genomic DNA at guanine and cytosine residues. MDP1 is generally a negative regulator of gene expression (17) that participates in the slow growth rate of mycobacteria (18). Expression of this protein is enhanced in both stationary and dormant mycobacteria (19, 20).

In this study, we describe for the first time that MDP1 negatively regulates KatG expression, which, in turn, causes phenotypic tolerance to INH. The current study describes a novel molecular mechanism by which phenotypic drug tolerance is acquired in mycobacteria. This mechanism may strongly impact our understanding of phenotypic tolerance to INH in *M. tuberculosis*.

EXPERIMENTAL PROCEDURES

Bacterial Strains and Antimicrobial Agents—Mycobacterium smegmatis mc^2155 (WT) and its histone-like protein/MDP1-deficient strain (MDP1-KO) were kindly provided by Dr. Thomas Dick (Novartis Institute for Tropical Diseases). An MDP1-complemented strain (MDP1-Comp) was generated previously (21). All *M. smegmatis* strains were cultured in Luria-Bertani (LB) broth or on LB agar plates (Sigma) aerobically at 37 °C on a magnetic stirrer set to rotate at 130 rpm. *Mycobacterium bovis* BCG strains were cultured in 7H9 broth base (Becton Dickinson and Company) supplemented with glycerol, 10% albumin-dextrose-catalase (ADC), and 0.05% Tween 80 (7H9-ADC-Tween), or on 7H11 agar plates supplemented with oleic acid, albumin, dextrose, and catalase (OADC). Ethambutol, rifampin, levofloxacin, and INH were purchased from Sigma. Rifampin was dissolved in ethanol, whereas levofloxacin, INH, and ethambutol were dissolved in distilled water. Stock solutions of each drug were filter-sterilized through 0.2-μm pore-size polyethersulfone membrane filters (Iwaki) except for rifampin, which was dissolved in ethanol.

Broth Microdilution—For the estimation of the minimum inhibitory concentrations (MICs) of each antibiotic, we used the broth microdilution method as previously described (22). Briefly, serial 2-fold dilutions of compounds were added to LB broth (for *M. smegmatis*) or 7H9-ADC-Tween (for BCG) to achieve final concentrations ranging from 128 – 0.125 μg/ml. The diluted antibiotic was then dispensed into the wells of microdilution plates at 0.1 ml per well. Aliquots of mycobacterial cells were then inoculated to a final concentration of ~10^4 CFU/well. After incubation at 37 °C for 4 days (*M. smegmatis*) or 14 days (BCG), the MICs were determined as the lowest concentrations of compound that prevented visible growth.

Cell Viability against INH—M. smegmatis and BCG cells were grown aerobically at 37 °C in liquid medium under appropriate conditions for 2–6 days. At each time point, an aliquot of each culture was withdrawn and adjusted to an optical density at 600 nm (A_{600}) of 0.1 and subsequently diluted 1:100 in fresh medium. After addition of INH solution to a final concentration of 6.25 μg/ml (for *M. smegmatis*) or 0.125 μg/ml (for BCG), cells were grown aerobically at 37 °C for 24 h (*M. smegmatis*) or for 48 h (BCG). Serial 10-fold dilutions of the cell suspensions were plated on agar plates to estimate the number of viable bacteria in the inoculum. After incubation for 4 days (*M. smegmatis*) or 14 days (BCG) at 37 °C, colonies were counted, and the proportion growing in the presence of various drug concentrations was compared with the total number of viable bacteria in the inoculum.

RNA Extraction—Cells were suspended in 1 ml of TRIzol reagent (Invitrogen) and disrupted using a Mini-BeadBeater. After incubation for 5 min at room temperature, 0.2 ml of chloroform was added, and the samples were shaken vigorously for 15 s. Cell lysates were centrifuged at 12,000 × *g* for 10 min at 4 °C, and the colorless upper aqueous phases were transferred to fresh tubes. Total RNA in the aqueous phase was precipitated by mixing samples with isopropyl alcohol followed by centrifugation. The pellets were washed with 75% ethanol, dried, and resuspended in 100 μl of diethylpyrocarbonate-treated dH_2O.

To remove the chromosomal DNA, samples were processed with a TURBO DNA-free kit (Applied Biosystems) according to the manufacturer's instructions. RNA quantification was performed by spectrophotometry using a NanoDrop 3300 (Thermo Scientific).

Microarray Analysis—A customized high-density oligonucleotide whole genome expression array (NimbleGen Systems) was designed for *M. smegmatis* mc^2155 using the genome sequence and ORF predictions available from the J. Craig Venter Institute. Total RNA was extracted from *M. smegmatis* WT and MDP1-KO cells in the exponential phase ($A_{600} \sim 0.8$). The cDNA synthesis, hybridization, and scanning were performed by NimbleGen Systems. Microarray data analysis was performed using GeneSpring GX (Agilent Technologies). The data presented are the results from one experiment.

Real-time Quantitative RT-PCR (qRT-PCR)—To confirm the results of microarray analysis, qRT-PCR was performed using Power SYBR green (Applied Biosystems). To generate cDNA samples, equal amounts of RNA were reverse transcribed using the High-capacity reverse transcription kit (Applied Biosystems) according to the manufacturer's instructions. Primers were designed using Primer Express software (version 2.0; Applied Biosystems), and the sequences of the primers used were as follows: *sigA* (forward), 5′-CGTTCCTCGACCTCATCCA-3′; *sigA* (reverse), 5′-GCCCTTGGTGTAGTCGAACTTC-3′; *katG* (forward), 5′-GACCGCGAATGACCTTGTGT-3′; and *katG* (reverse), 5′-TGTCGGACTGGGCATAAACC-3′. A standard curve was generated for relative quantification of the PCR products, and a control reaction lacking reverse transcriptase was performed for every RNA sample. The major housekeeping σ factor gene, *sigA*, was used to normalize mRNA levels. Analysis was performed on triplicate biological samples that were each assayed in triplicate.

Western Blotting—Mycobacterial cells were grown at 37 °C and harvested at the indicated time points. To obtain whole-cell protein extracts, cells were washed three times with PBS and disrupted using a Mini-BeadBeater as described previously (23). Quantities of protein were determined by the Bradford assay (24) using the Bio-Rad protein assay kit (Bio-Rad). The same amount of total protein from each strain (2 μg per well) was separated by SDS-PAGE. Immunoblotting was carried out after SDS-PAGE and transfer of proteins to a PVDF membrane by incubation with anti-MDP1 and anti-KatG antibodies, as described previously (25). Anti-heat shock protein Hsp65 (GroEL2) antibody was used as a loading control (26, 27). The expression levels of different proteins were analyzed using the public domain software Image J (a Java image processing program developed by the National Institutes of Health Image for Macintosh).

Reduction of Nitroblue Tetrazolium (NBT)—This test detects INH activation by KatG and is dependent on the reduction of NBT by superoxide-free radical in the presence of INH to form an insoluble formazan. Reduction was monitored qualitatively following electrophoresis of whole-cell extracts on native gels, as described previously (28). Before samples were subjected to native PAGE, protein concentrations were quantified by Bradford assay. The gel was soaked in 50 ml of 50 mM sodium phosphate (pH 7.0) containing 68 mg of INH, 12.5 mg of NBT, and 15 ml of 30% H_2O_2. Color development was complete after 30 min. The gel was then rinsed with distilled water and soaked in 7% acetic acid, 1% glycerol in distilled water before visualization. The levels of KatG activity in each strain observed in the native PAGE gel were also analyzed using ImageJ software.

Transformation and Isolation of Recombinant M. bovis BCG Strains—Preparation of *M. bovis* BCG competent cells and electroporation procedures were performed according to standard procedures (29). Briefly, *M. bovis* BCG strain Tokyo was grown in 7H9-OADC-Tween until an A_{600} of 0.6 was reached. Cells were harvested by centrifugation, washed several times, and resuspended in one-tenth of their original volume of 10% glycerol to obtain competent cells. The MDP1-antisense plasmid (18) as well as the empty vector, pMV261, were introduced into BCG-competent cells using a Gene pulser II (Bio-Rad) with the following settings: 2.5 kV, 129 ohms, 50 μF. After electroporation, cells were resuspended in 4 ml of 7H9-ADC-Tween and incubated for 20 h at 37 °C. Following incubation, appropriate dilutions were added to 7H11 agar containing 10 μg/ml kanamycin. One clone of empty vector transformant (pMV261) and two clones of transformants carrying MDP1-antisense plasmid (pAS-MDP1-1 and pAS-MDP1-2) were chosen for further analysis.

Expression and Purification of Recombinant MDP1—Recombinant MDP1 was obtained as described previously (30). Briefly, the oligonucleotide primers (forward, 5′-CCCCATATGAACAAAGCAGAGCTCATTGAC-3′; reverse, 5′-CCCAAGCTTTTTGCGACCCCGCCGAGCGG-3′) were synthesized based on the nucleotide sequences of BCG and *M. tuberculosis mdp1*. The amplified DNA fragment were digested with NdeI and HindIII, cloned into the same sites of pET22b+ (Novagen, Darmstadt, Germany), and introduced into *Escherichia coli* BL21(DE3). Expression of recombinant protein was induced by addition of 0.1 mM isopropyl-1-thio-β-D-galactopyranoside, and the cells were then incubated for 10 h at 22 °C. After incubation, cells were disrupted, and the supernatant was collected by centrifugation 8,000 × *g* for 30 min. After filtering the supernatant through a 0.22-μm membrane, it was applied to a 1-ml Hi-Trap chelating column charged previously with 100 mM $NiSO_4$ and equilibrated with 20 mM sodium phosphate, pH 7.4, 10 mM imidazole, and 0.5 M NaCl. After washing out unbound proteins, the protein was eluted with the same buffer containing 300 mM imidazole. The fractions containing MDP1 were collected and dialyzed against PBS. The purity of the protein was confirmed by staining as a single band with Coomassie Brilliant Blue R-250 following separation by SDS-PAGE.

Electrophoretic Mobility Shift Assay (EMSA)—Primers (forward, 5′-CTCTGACAGGCGCCAATGCG-3′; reverse, 5′-GACCAGAAGGCTACTGCTTT-3′) were used to amplify a 80-bp fragment containing the *furA* promoter region, as described by Milano *et al.* (31). The amplified DNA fragment was labeled with digoxigenin with a digoxigenin gel shift kit, second generation (Roche Diagnostics), according to the manufacturer's protocol. EMSA was also performed using the same kit according to the manufacturer's instructions. Briefly, purified recombinant MDP1 protein was incubated with 40 fg of digoxigenin-labeled double-stranded DNA fragments in a final volume of 25 μl. Incubations were carried out at 4 °C for 2 h in a solution of 10

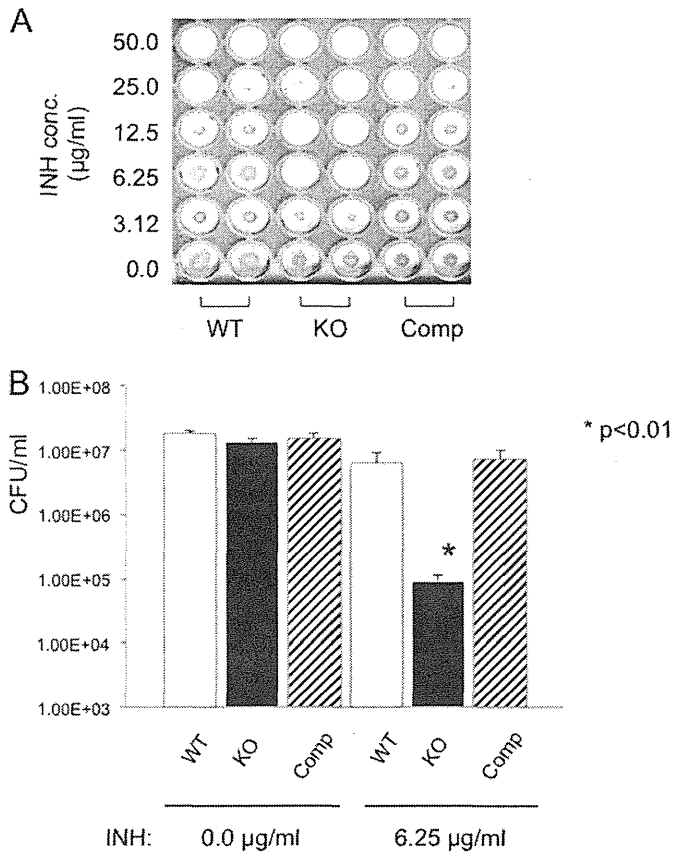

FIGURE 1. **Comparison of the INH susceptibilities of *M. smegmatis* WT, MDP1-KO and MDP1-Comp.** *A*, broth microdilution method. INH susceptibilities were analyzed by inoculating each bacterial strain in 7H9-ADC-Tween culture medium containing serially diluted INH. *B*, comparison of CFU count. Each strain was exposed to INH at a concentration below the MIC. After incubation for 48 h, cell suspensions were inoculated onto LB agar to estimate the number of viable bacteria in the inoculum. MDP1-KO CFUs (*solid bar*) decreased markedly after exposure to INH compared with WT (open bar) and MDP1-Comp (*hatched bar*) CFUs. Mean values and S.E. for three experiments are shown. *conc.*, concentration.

mM Tris-HCl (pH 7.6), 50 mM NaCl, 5% (v/v) glycerol, 1 mM EDTA, and 1 mM DTT. For the competition assay, unlabeled oligonucleotide was added to a 100-fold excess. The reaction mixtures were loaded onto 6% polyacrylamide gels that were pre-electrophoresed at 100 V for 1 h in 1× Tris borate-EDTA buffer consisting of 89 mM Tris, 89 mM borate, and 2 mM EDTA (pH 8.3). Polyacrylamide gels were electrophoresed at 100 V at ambient temperature until the bromphenol blue dye front reached the bottom. The probes were transferred onto a positively charged nylon membrane (Roche Diagnostics) and detected according to the kit protocol.

RESULTS

MDP1-deficient M. smegmatis Showed Increased Susceptibility to INH—To determine whether MDP1 is involved in the acquisition of drug sensitivity in mycobacteria, we analyzed the susceptibility of *M. smegmatis* WT, MDP1-KO, and MDP1-Comp cells to antibiotics. As shown in Fig. 1*A*, a marked increase in susceptibility to INH was observed in MDP1-KO cells. We determined the MICs of INH for each strain using the broth microdilution method described previously (32). As presented in Table 1, the MIC of MDP1-KO cells was 8.0 μg/ml,

TABLE 1
MICs against various antibiotics by the broth microdilution method
EB, ethambutol; RFP, rifampin; LVFX, levofloxacin.

	EB	RFP	LVFX	INH
	μg/ml	*μg/ml*	*μg/ml*	*μg/ml*
WT	1.0	8	0.5	32
KO	1.0	8	0.5	8
Comp	1.0	8	0.5	32

TABLE 2
Expression of genes related to INH resistance analyzed by microarray

	WT	MDP1-KO
MSMEG_3461 (*katG*)	2.910772	6.552576
MSMEG_3151 (*inhA*)	3.056271	2.7222855
MSMEG_4891 (*ahpC*)	164.84808	168.63435

whereas the MICs for the other strains were 4-fold higher. In contrast, *M. smegmatis* WT, MDP1-KO, and MDP1-Comp were equally susceptible to the other drugs tested, including ethambutol, rifampin, and levofloxacin (Table 1).

To clarify the effects of culture medium components on susceptibility to antibiotics, we performed broth microdilution assays using 7H9-ADC-Tween as the culture medium. The MICs of each strain in 7H9-ADC-Tween were the same as those in LB broth (data not shown). To confirm the differential susceptibility to INH between strains, we counted the CFUs in each strain after exposure to INH at a concentration below the MIC for MDP1-KO cells (Fig. 1*B*). We found that MDP1-KO cells showed decreased viability following treatment with INH compared with WT and MDP1-Comp cells. These results suggested that susceptibility to INH is affected by the presence of MDP1 in *M. smegmatis* cells. Our results are consistent with the data recently reported by Dahl *et al.* (33).

Increased Transcription of katG in MDP1-KO—To investigate the effect of MDP1 on the expression of genes related to INH resistance, we performed DNA microarray analysis to compare gene expression profiles between *M. smegmatis* WT and MDP1-KO strains. The expression levels of the genes related to INH resistance, such as *inhA* and *ahpC*, were similar in MDP1-KO and WT cells (Table 2). However, a significant increase in *katG* expression was observed in MDP1-KO cells.

To confirm the increased *katG* transcription in MDP1-KO cells, total RNA from *M. smegmatis* WT, MDP1-KO, and MDP1-Comp cells was isolated and used for qRT-PCR analysis of *katG* expression. The expression levels of *katG* mRNA were determined by the comparative threshold cycle method and then normalized to *sigA* expression. As expected, MDP1-KO cells possessed a 2-fold higher expression level of *katG* mRNA compared with WT cells (Fig. 2). In contrast, MDP1-Comp cells exhibited 2-fold lower *katG* expression than the WT strain, whereas the viability of MDP1-Comp cells treated with INH was similar to that of WT cells.

Increased KatG Protein Expression in MDP1-KO—To support the results of DNA microarrays and qRT-PCR, Western blotting was used to analyze the expression level of KatG protein. As a loading control, anti-Hsp65 antibody was used to confirm that the protein concentrations were equal in all samples. The results demonstrated that *M. smegmatis* WT and MDP1-Comp cells produced similar amounts of KatG, whereas KatG expression was increased in MDP1-KO cells (Fig. 3*A*).

These data suggest that MDP1 regulates the KatG protein level in *M. smegmatis* cells.

Enhanced Activation of INH in MDP1-KO Cells—Next, we investigated whether INH activation is increased in MDP1-KO cells, which produce larger amounts of KatG than WT cells (Fig. 3*A*). The INH-dependent NBT reduction assay is commonly used to estimate the level of INH activation by KatG because the KatG enzyme produces free radicals upon activation of INH (34, 35).

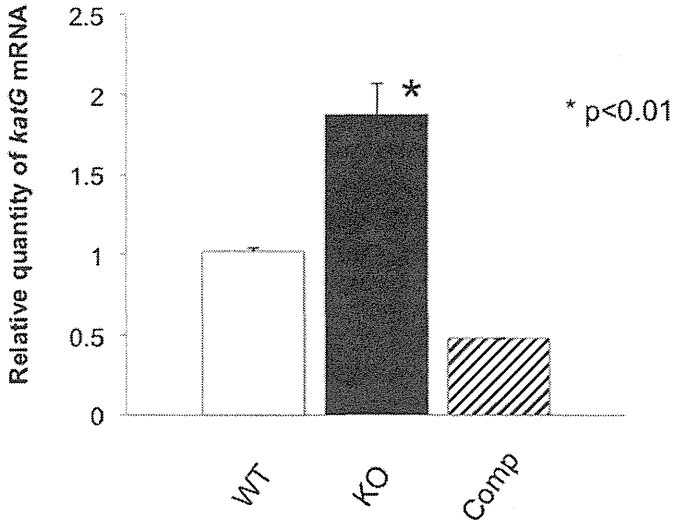

FIGURE 2. **Analysis of *katG* expression by qRT-PCR.** Transcription of *katG* was quantified by qRT-PCR. The relative expression levels of *katG* in MDP1-KO (*solid bar*) and MDP1-Comp (*hatched bar*) cells were compared with that in WT cells (*open bar*) after normalization to the housekeeping gene, *sigA*. The cDNA level is expressed as the average of three replicates. For statistical analysis, one-way ANOVA test was used to obtain the *p* value. *, $p < 0.01$.

The NBT reduction assay was performed using cell lysates derived from *M. smegmatis* WT, MDP1-KO, and MDP1-Comp cells. A single band of activity was detected in each lane at the same distance on the gel as a purple formazan product. As shown in Fig. 3*B*, whole-cell lysates of MDP1-KO cells exhibited a higher capacity to reduce NBT to formazan in the presence of INH than other strains. To confirm that the different NBT-reducing activities between strains were due to different KatG expression levels in each strain and not to amino acid substitutions, we compared their *katG* nucleotide sequences and found no amino acid substitutions (data not shown). These data suggest that increased expression of KatG results in the activation of INH, and consequently, MDP1-KO cells are less viable following treatment with INH.

MDP1 Affects INH Susceptibility in Growth Phase-dependent Manner—Our previous study revealed that the expression of MDP1 is up-regulated in the stationary phase of mycobacterial culture (21). Therefore, we investigated whether the different expression levels of MDP1 during different growth states produced the INH-resistant phenotype in *M. smegmatis*. The expression of MDP1 was shown to increase in both WT and MDP1-Comp cells during the stationary growth phase (day 6 in Fig. 4). In contrast, expression of KatG was observed during the

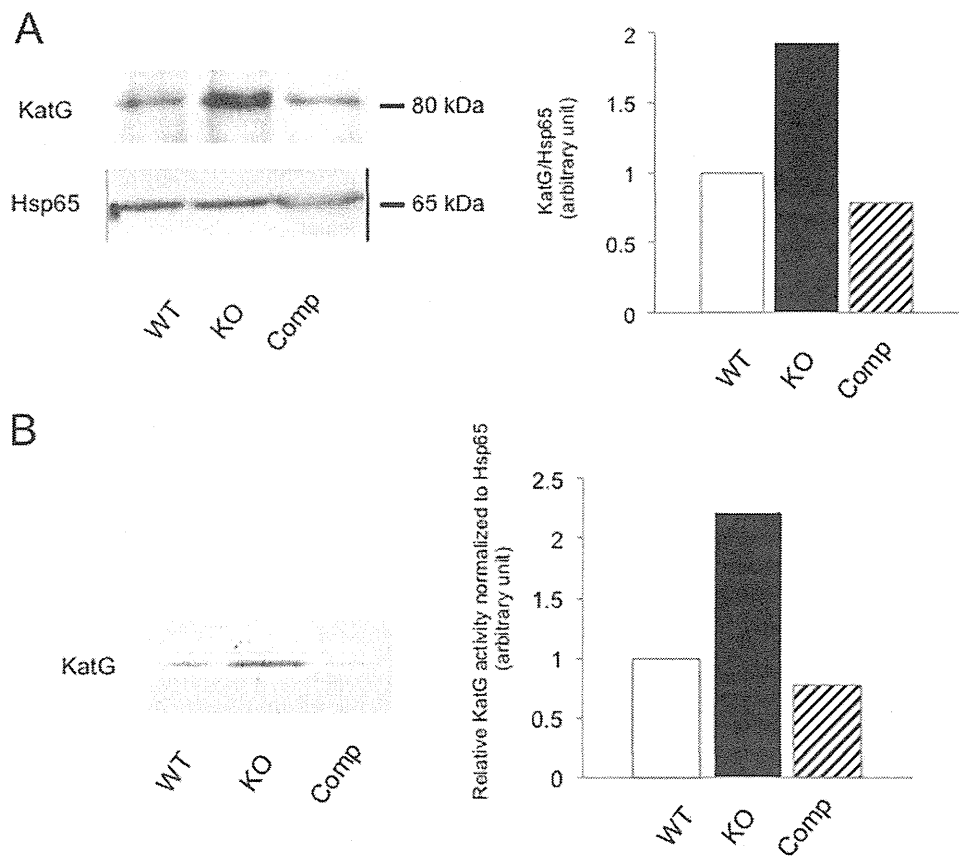

FIGURE 3. **Influence of MDP1-deficiency on KatG protein expression and INH activation.** *M. smegmatis* wild-type (WT), MDP1-KO (KO), and MDP1-Comp (Comp) cells were grown at 37 °C for 48 h. *A*, KatG expression was analyzed by Western blotting using rabbit anti-KatG antibodies. *B*, the level of activation of INH by KatG in each strain was estimated by NBT reduction assay. INH-dependent reduction of NBT to formazan was monitored on a native PAGE gel.

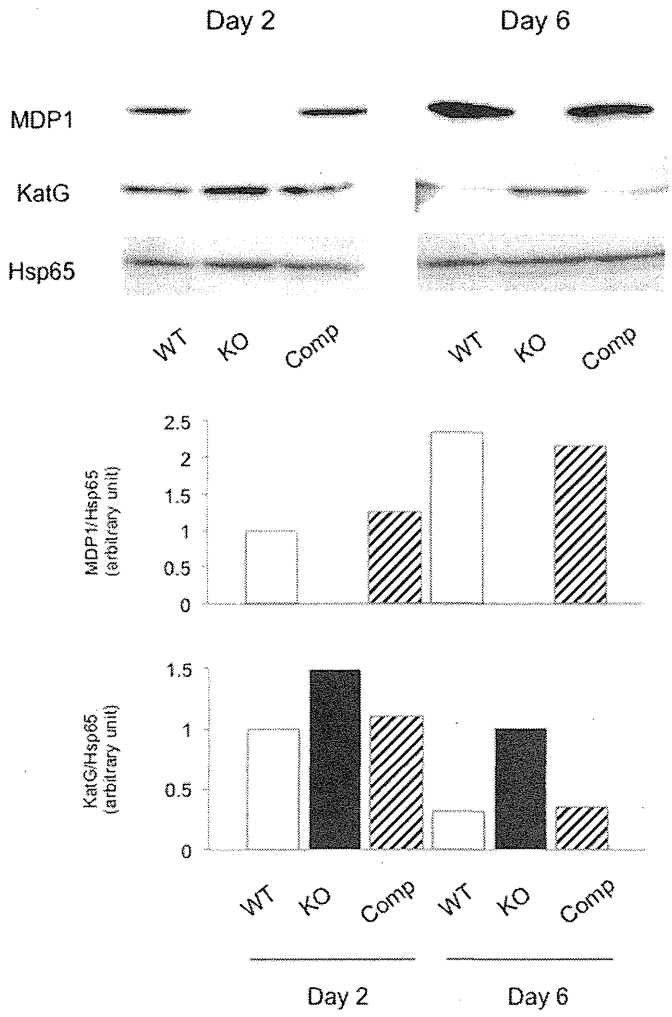

FIGURE 4. **Expression of MDP1 and KatG proteins during the logarithmic and stationary growth phases in *M. smegmatis*.** Analysis of the expression of MDP1 and KatG during the logarithmic (day 2) and stationary (day 6) growth phases was performed by Western blotting. WT, *M. smegmatis*; *KO*, WT MDP1-KO; *Comp*, MDP1-Comp.

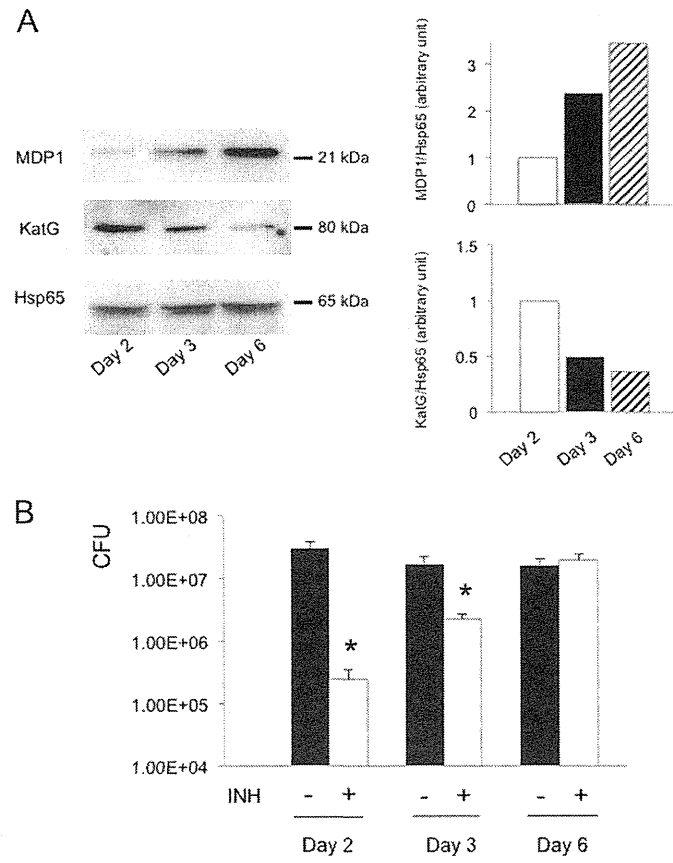

FIGURE 5. **Growth phase-dependent expression of MDP1 and KatG and susceptibility to INH in *M. smegmatis* WT.** *A*, the expression levels of MDP1 and KatG were monitored by Western blotting on days 2, 3, and 6. *B*, INH susceptibility was analyzed by CFU assay. Initially, *M. smegmatis* WT cells were grown at 37 °C in LB broth without INH. On days 2, 3, and 6, cells were collected and exposed to INH at a concentration of 0.0 μg/ml or 6.25 μg/ml for 2 days. After INH treatment, the drug was removed from the culture media, and cells were diluted and plated onto INH-free LB agar plates. The number of viable cells obtained following treatment with INH (*open bar*) was compared with the number obtained without INH treatment (*solid bar*) at each time point. Mean values and S.E. for three experiments are shown. The statistical significance of the differences in CFUs between the different time points was determined by one-way ANOVA. *, $p < 0.01$.

logarithmic growth phase in both WT and MDP1-Comp cells but diminished during the stationary growth phase (Fig. 4). MDP1-KO cells, however, showed enhanced KatG expression during the logarithmic growth phase (Fig. 2), whereas KatG was still expressed even in the stationary growth phase (Fig. 4).

A time course analysis was performed investigating the expression levels of MDP1 and KatG and the INH susceptibility of *M. smegmatis* WT cells. Western blotting revealed a time-dependent up-regulation of MDP1 expression, whereas the expression of KatG was inversely decreased (Fig. 5*A*). Cell viability in the presence of INH was also found to vary at each time point. On day 2 (exponential phase), a significant reduction in the number of CFUs was observed after treatment with INH at a concentration of 6.25 μg/ml, whereas most of the cells survived exposure to INH at the same concentration on day 6 (stationary phase) (Fig. 5*B*). These results revealed that the acquisition of INH tolerance occurred in a time-dependent manner and was positively correlated with increased MDP1 expression.

MDP1 Affects INH Susceptibility of M. bovis BCG—To clarify whether MDP1 influences the susceptibility of other mycobacterial species to INH, drug sensitivity was measured in two *M. bovis* BCG clones carrying the MDP1-antisense plasmid (pAS-MDP1-1 and pAS-MDP1-2) and the reference strain (pMV261). *M. bovis* BCG is an attenuated strain of *M. bovis* that belongs to the *M. tuberculosis* complex. The architecture of the *katG* gene and its upstream regulatory region are the same in *M. bovis* BCG and *M. tuberculosis*. Western blotting showed that MDP1 expression was decreased by half, and KatG expression was increased >2-fold, in both pAS-MDP1-1 and pAS-MDP1-2 compared with pMV261 (Fig. 6*A*). We then determined the MICs of these strains in the presence of INH and found that mutants with reduced MDP1 expression showed increased susceptibility to INH, consistent with data obtained for *M. smegmatis* MDP1-KO (Figs. 6 and 7). These results suggest that MDP1 influences the susceptibility of not only the avirulent rapidly growing *M. tuberculosis* complex but also the slow growing *M. tuberculosis* complex to INH.

MDP1 Binds to DNA Sequence in FurA-KatG Promoter Region—A previous report revealed that *katG* is negatively regulated by FurA, a homologue of the ferric uptake regulator Fur, by binding to its promoter region (36). It was also shown that

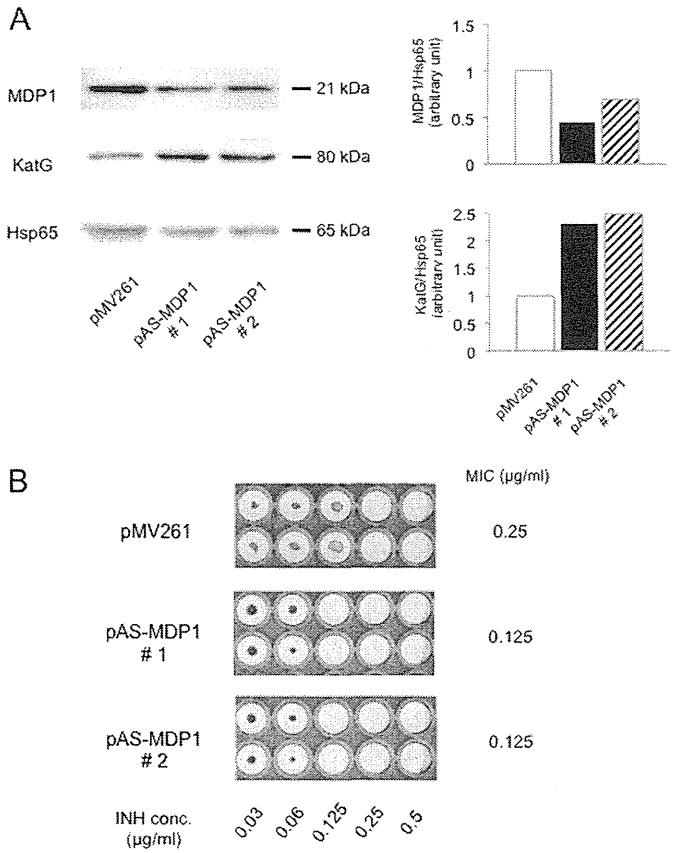

FIGURE 6. **MDP1 affects the expression of KatG protein and INH susceptibility in *M. bovis* BCG.** *A*, comparison of MDP1 and KatG expression in two *M. bovis* BCG clones carrying the MDP1-antisense plasmid and a reference strain. BCG cells were grown at 37 °C for 10 days. MDP1-antisense plasmids (pAS-MDP1−1 and −2) reduced the expression of MDP1 compared with the control plasmid (pMV261). *B*, comparison of the INH susceptibility of the two *M. bovis* BCG clones carrying MDP1-antisense plasmids and the reference strain. The effect of INH was monitored by the broth microdilution method. *conc.*, concentration.

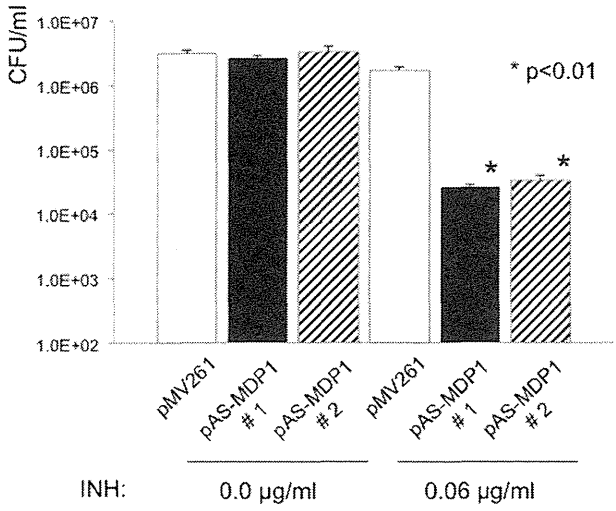

FIGURE 7. **CFU assay to estimate the INH susceptibility of recombinant BCG harboring the MDP1 antisense plasmid.** Knockdown of MDP1 expression by antisense production (*solid* and *hatched bars*) in BCG revealed increased susceptibility of the bacterial cells to INH compared with recombinant BCG harboring the control plasmid (*open bar*) in the presence of 0.125 μg/ml INH for 48 h. Mean values and S.E. for three experiments are shown. The statistical significance of the differences in CFUs between the different time points was determined by one-way ANOVA. *, $p < 0.01$.

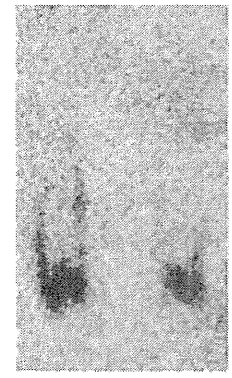

FIGURE 8. **Gel-shift assay to analyze the interaction between MDP1 and the *furA-katG* DNA promoter region.** Recombinant MDP1 was incubated with either digoxigenin (*DIG*)-labeled DNA probes including the sequence of the *furA-katG* promoter region alone, or together with a 100-fold weight excess of non-digoxigenin labeled probes. *Left lane*, digoxigenin-labeled probes alone. *Middle lane*, digoxigenin-labeled probes co-incubated with recombinant MDP1 protein. *Right lane*, digoxigenin-labeled probes co-incubated with recombinant MDP1 in the presence of an excess of the non-digoxigenin-labeled probes.

furA and *katG* are co-transcribed from a common regulatory region located immediately upstream of the *furA* gene (31). Furthermore, inactivation of *furA* resulted in *katG* up-regulation, which increased the sensitivity of mycobacterial cells to INH (7). We hypothesized that MDP1 may directly bind to the promoter region of the FurA-KatG operon and performed gel-shift assays to test the hypothesis. We observed that co-incubation of MDP1 with a digoxigenin-labeled DNA fragment containing the *furA-katG* promoter region resulted in the disappearance of a DNA band. This was due to altered electrophoretic mobility of the MDP1-DNA complex because of the high basic charge of MDP1 (pI = 12.4). We confirmed the specificity of this binding by showing the absence of a band shift in the presence of non-digoxigenin-labeled competitor (Fig. 8). These data show that MDP1 has the ability to bind to the *furA-katG* promoter region.

DISCUSSION

MDPI is a conserved histone-like DNA binding protein found in mycobacteria including *M. tuberculosis*, *Mycobacterium leprae*, and *M. smegmatis*. Because chromatin-associated proteins are thought to organize the bacterial chromosome and exert a regulatory influence on transcription, recombination and DNA replication (37), it has been postulated that MDP1 may contribute to the regulation of gene expression. In this study, we found that MDP1 down-regulates the expression of KatG in mycobacteria.

KatG is an antioxidant enzyme that converts hydrogen peroxide (H_2O_2) into water and oxygen via its catalase activity (38, 39). Because mycobacteria encounter oxidative stress inside host cells, antioxidant proteins such as KatG play a significant role in intracellular survival. Sherman *et al.* (40) reported that INH-resistant *katG* mutants acquired a second mutation

resulting in hyperexpression of alkyl hydroperoxidase (AhpC) to compensate for the loss of KatG activity in the detoxification of organic peroxides. However, overexpression of AhpC did not result in increased *M. tuberculosis* survival, and deletion of *ahpC* did not alter the expression of *katG*. Thus, AhpC does not compensate for the loss of KatG activity. In addition to DNA-binding activity, we discovered recently that MDP1 enzymatically converts H_2O_2 into water and oxygen in the presence of Fe^{2+} (41). Therefore, it is conceivable that both KatG and MDP1 play a significant role in H_2O_2 detoxification in mycobacterial cells. MDP1 rather than AhpC may compensate for reduced KatG activity, and therefore their expression levels are reciprocally regulated.

It is also known that *katG* is regulated negatively by FurA, a homologue of the ferric uptake regulator Fur, which is encoded by a gene located immediately upstream of *katG* (36). Similar to FurA, MDP1 has affinity to iron (41), and the expression levels of both FurA and MDP1 are influenced by the environmental iron concentration (42). EMSA assay revealed that MDP1 has an actual capacity to bind to the promoter region of *furA-katG*, suggesting that MDP1 is a trans-acting factor that regulates the transcription of the FurA-KatG operon by directly binding to its promoter region. Future studies, including chromatin immunoprecipitation assays, will clarify the effect of MDP1 on the *furA-katG* genomic region.

Drug tolerance is a phenomenon seen in many microorganisms during their growth *in vivo* (3, 43, 44). It is known that phenotypic tolerance occurs when the environmental or physiological status of the bacteria change. For example, environmental factors such as low pH (45), depletion of certain nutrients (46), and high magnesium or calcium concentration (47) induce phenotypic tolerance. The inhibition of growth occurs in the stationary phase and is the most common cause of reduced drug susceptibility in all bacteria (48).

It has been reported that the expression of histone-like proteins varies with the age of the culture. For example, Fis is a cofactor in a site-specific recombination system that is expressed at a high level in the early exponential phase of *E. coli* growth (49). In contrast, integration host factor is found to be most abundant when the culture enters the stationary phase (50). Because the expression of MDP1 is enhanced in the stationary growth phase (20), this molecule may affect the gene profile of cells in the stationary phase. The current study shows that alteration of MDP1 expression induces growth phase-dependent tolerance to INH by controlling KatG expression in *M. smegmatis*. A schematic diagram showing a hypothetical mechanism of INH tolerance regulated by MDP1 is provided in Fig. 9. To our knowledge, this is the first description of a molecular mechanism underlying growth phase-dependent tolerance to INH in mycobacteria.

Regulation of KatG expression appears to be conserved in several mycobacteria, including *M. tuberculosis* and *M. smegmatis* (31). We show here that reduction of MDP1 expression by antisense knockdown increases the sensitivity of *M. bovis* BCG to INH (Fig. 7). *M. bovis* BCG and *M. tuberculosis* show similar susceptibilities to INH, and the DNA sequences of their *katG* genes and upstream regulatory regions are identical. Taken together, MDP1 may affect the expression level of KatG

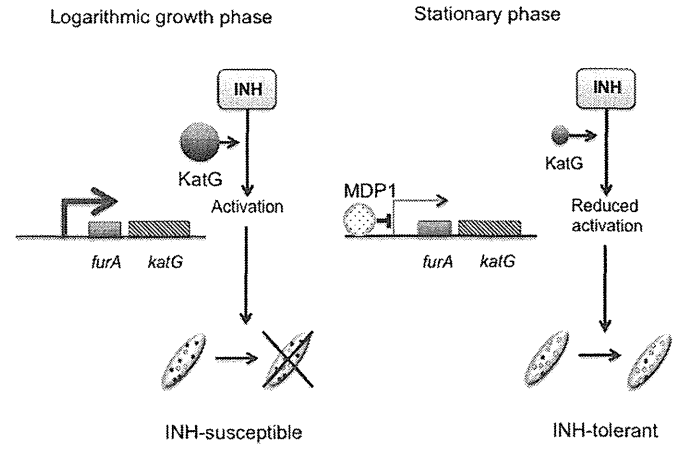

FIGURE 9. **Schematic diagram showing the hypothetical mechanism of INH tolerance regulated by MDP1.** INH is a prodrug that is converted to an activated, bactericidal form by the enzymatic activity of KatG. In the logarithmic growth phase, cells expressing KatG show susceptibility to INH. In contrast, up-regulation of MDP1 expression occurs in cells during the stationary phase, which leads to suppression of KatG expression probably by direct binding of MDP1 to the *furA-katG* promoter region. Thus, cells with reduced KatG activity become phenotypically tolerant to INH.

and the susceptibility of pathogenic *M. tuberculosis* to INH. Our data suggest that the artificial reduction of MDP1 expression may enhance the efficacy of INH and shorten the length of tuberculosis chemotherapy against both active and latent diseases.

Acknowledgments—We are grateful to Dr. Thomas Dick (Novartis Institute for Tropical Diseases) for providing Ms-MDP1/HLP-KO M. smegmatis. We also thank Sara Matsumoto and Chihiro Inoue for assistance with the experiments and encouragement.

REFERENCES

1. Ormerod, L. P. (2008) The evidence based treatment of tuberculosis: Where and why are we failing? *Thorax* **63,** 388–390
2. Nachega, J. B., and Chaisson, R. E. (2003) Tuberculosis drug resistance: A global threat. *Clin. Infect. Dis.* **36,** S24–30
3. Wallis, R. S., Patil, S., Cheon, S. H., Edmonds, K., Phillips, M., Perkins, M. D., Joloba, M., Namale, A., Johnson, J. L., Teixeira, L., Dietze, R., Siddiqi, S., Mugerwa, R. D., Eisenach, K., and Ellner, J. J. (1999) Drug tolerance in *Mycobacterium tuberculosis*. *Antimicrob. Agents Chemother.* **43,** 2600–2606
4. Vilchèze, C., and Jacobs, W. R., Jr. (2007) The mechanism of isoniazid killing: Clarity through the scope of genetics. *Annu. Rev. Microbiol.* **61,** 35–50
5. Herbert, D., Paramasivan, C. N., Venkatesan, P., Kubendiran, G., Prabhakar, R., and Mitchison, D. A. (1996) Bactericidal action of ofloxacin, sulbactam-ampicillin, rifampin, and isoniazid on logarithmic- and stationary-phase cultures of *Mycobacterium tuberculosis*. *Antimicrob. Agents Chemother.* **40,** 2296–2299
6. Zhang, Y., Heym, B., Allen, B., Young, D., and Cole, S. (1992) The catalase-peroxidase gene and isoniazid resistance of *Mycobacterium tuberculosis*. *Nature* **358,** 591–593
7. Pym, A. S., Domenech, P., Honoré, N., Song, J., Deretic, V., and Cole, S. T. (2001) Regulation of catalase-peroxidase (KatG) expression, isoniazid sensitivity, and virulence by furA of *Mycobacterium tuberculosis*. *Mol. Microbiol.* **40,** 879–889
8. Banerjee, A., Dubnau, E., Quemard, A., Balasubramanian, V., Um, K. S., Wilson, T., Collins, D., de Lisle, G., and Jacobs, W. R., Jr. (1994) inhA, a gene encoding a target for isoniazid and ethionamide in *Mycobacterium tuberculosis*. *Science* **263,** 227–230

9. Dessen, A., Quémard, A., Blanchard, J. S., Jacobs, W. R., Jr., and Sacchettini, J. C. (1995) Crystal structure and function of the isoniazid target of *Mycobacterium tuberculosis*. *Science* **267,** 1638–1641
10. Quémard, A., Sacchettini, J. C., Dessen, A., Vilcheze, C., Bittman, R., Jacobs, W. R., Jr., and Blanchard, J. S. (1995) Enzymatic characterization of the target for isoniazid in *Mycobacterium tuberculosis*. *Biochemistry* **34,** 8235–8241
11. Wilson, T. M., and Collins, D. M. (1996) ahpC, a gene involved in isoniazid resistance of the *Mycobacterium tuberculosis* complex. *Mol. Microbiol.* **19,** 1025–1034
12. Miesel, L., Weisbrod, T. R., Marcinkeviciene, J. A., Bittman, R., and Jacobs, W. R., Jr. (1998) NADH dehydrogenase defects confer isoniazid resistance and conditional lethality in *Mycobacterium smegmatis*. *J Bacteriol* **180,** 2459–2467
13. Mdluli, K., Slayden, R. A., Zhu, Y., Ramaswamy, S., Pan, X., Mead, D., Crane, D. D., Musser, J. M., and Barry, C. E., 3rd (1998) Inhibition of a *Mycobacterium tuberculosis* β-ketoacyl ACP synthase by isoniazid. *Science* **280,** 1607–1610
14. Larsen, M. H., Vilchèze, C., Kremer, L., Besra, G. S., Parsons, L., Salfinger, M., Heifets, L., Hazbon, M. H., Alland, D., Sacchettini, J. C., and Jacobs, W. R., Jr. (2002) Overexpression of inhA, but not kasA, confers resistance to isoniazid and ethionamide in *Mycobacterium smegmatis*, *M. bovis* BCG, and *M. tuberculosis*. *Mol. Microbiol.* **46,** 453–466
15. Ando, H., Kitao, T., Miyoshi-Akiyama, T., Kato, S., Mori, T., and Kirikae, T. (2011) Down-regulation of katG expression is associated with isoniazid resistance in *Mycobacterium tuberculosis*. *Mol. Microbiol.* **79,** 1615–1628
16. Colangeli, R., Helb, D., Vilchèze, C., Hazbón, M. H., Lee, C. G., Safi, H., Sayers, B., Sardone, I., Jones, M. B., Fleischmann, R. D., Peterson, S. N., Jacobs, W. R., Jr., and Alland, D. (2007) Transcriptional regulation of multi-drug tolerance and antibiotic-induced responses by the histone-like protein Lsr2 in M. tuberculosis. *PLoS Pathog.* **3,** e87
17. Matsumoto, S., Furugen, M., Yukitake, H., and Yamada, T. (2000) The gene encoding mycobacterial DNA-binding protein I (MDPI) transformed rapidly growing bacteria to slowly growing bacteria. *FEMS Microbiol. Lett.* **182,** 297–301
18. Lewin, A., Baus, D., Kamal, E., Bon, F., Kunisch, R., Maurischat, S., Adonopoulou, M., and Eich, K. (2008) The mycobacterial DNA-binding protein 1 (MDP1) from *Mycobacterium bovis* BCG influences various growth characteristics. *BMC Microbiol.* **8,** 91
19. Dick, T., Lee, B. H., and Murugasu-Oei, B. (1998) Oxygen depletion-induced dormancy in *Mycobacterium smegmatis*. *FEMS Microbiol. Lett.* **163,** 159–164
20. Matsumoto, S., Yukitake, H., Furugen, M., Matsuo, T., Mineta, T., and Yamada, T. (1999) Identification of a novel DNA-binding protein from *Mycobacterium bovis* Bacillus Calmette-Guérin. *Microbiol. Immunol.* **43,** 1027–1036
21. Katsube, T., Matsumoto, S., Takatsuka, M., Okuyama, M., Ozeki, Y., Naito, M., Nishiuchi, Y., Fujiwara, N., Yoshimura, M., Tsuboi, T., Torii, M., Oshitani, N., Arakawa, T., and Kobayashi, K. (2007) Control of cell wall assembly by a histone-like protein in Mycobacteria. *J. Bacteriol.* **189,** 8241–8249
22. Brown, B. A., Wallace, R. J., Jr., and Onyi, G. O. (1992) Activities of clarithromycin against eight slowly growing species of nontuberculous mycobacteria, determined by using a broth microdilution MIC system. *Antimicrob. Agents Chemother.* **36,** 1987–1990
23. Yuan, Y., Crane, D. D., Simpson, R. M., Zhu, Y. Q., Hickey, M. J., Sherman, D. R., and Barry, C. E., 3rd (1998) The 16-kDa α-crystallin (Acr) protein of *Mycobacterium tuberculosis* is required for growth in macrophages. *Proc. Natl. Acad. Sci. U.S.A.* **95,** 9578–9583
24. Bradford, M. M. (1976) A rapid and sensitive method for the quantitation of microgram quantities of protein utilizing the principle of protein-dye binding. *Anal. Biochem.* **72,** 248–254
25. Sekiguchi, J., Miyoshi-Akiyama, T., Augustynowicz-Kopeć, E., Zwolska, Z., Kirikae, F., Toyota, E., Kobayashi, I., Morita, K., Kudo, K., Kato, S., Kuratsuji, T., Mori, T., and Kirikae, T. (2007) Detection of multidrug resistance in *Mycobacterium tuberculosis*. *J. Clin. Microbiol.* **45,** 179–192
26. Blasco, B., Chen, J. M., Hartkoorn, R., Sala, C., Uplekar, S., Rougemont, J., Pojer, F., and Cole, S. T. (2012) Virulence regulator EspR of *Mycobacterium tuberculosis* is a nucleoid-associated protein. *PLoS Pathog.* **8,** e1002621
27. Ojha, A., Anand, M., Bhatt, A., Kremer, L., Jacobs, W. R., Jr., and Hatfull, G. F. (2005) GroEL1: A dedicated chaperone involved in mycolic acid biosynthesis during biofilm formation in mycobacteria. *Cell* **123,** 861–873
28. Hillar, A., and Loewen, P. C. (1995) Comparison of isoniazid oxidation catalyzed by bacterial catalase-peroxidases and horseradish peroxidase. *Arch. Biochem. Biophys.* **323,** 438–446
29. Zhang, Y., Lathigra, R., Garbe, T., Catty, D., and Young, D. (1991) Genetic analysis of superoxide dismutase, the 23-kilodalton antigen of *Mycobacterium tuberculosis*. *Mol. Microbiol.* **5,** 381–391
30. Aoki, K., Matsumoto, S., Hirayama, Y., Wada, T., Ozeki, Y., Niki, M., Domenech, P., Umemori, K., Yamamoto, S., Mineda, A., Matsumoto, M., and Kobayashi, K. (2004) Extracellular mycobacterial DNA-binding protein 1 participates in mycobacterium-lung epithelial cell interaction through hyaluronic acid. *J. Biol. Chem.* **279,** 39798–39806
31. Milano, A., Forti, F., Sala, C., Riccardi, G., and Ghisotti, D. (2001) Transcriptional regulation of furA and katG upon oxidative stress in *Mycobacterium smegmatis*. *J. Bacteriol.* **183,** 6801–6806
32. Wallace, R. J., Jr., Nash, D. R., Steele, L. C., and Steingrube, V. (1986) Susceptibility testing of slowly growing mycobacteria by a microdilution MIC method with 7H9 broth. *J. Clin. Microbiol.* **24,** 976–981
33. Whiteford, D. C., Klingelhoets, J. J., Bambenek, M. H., and Dahl, J. L. (2011) Deletion of the histone-like protein (Hlp) from *Mycobacterium smegmatis* results in increased sensitivity to UV exposure, freezing, and isoniazid. *Microbiology* **157,** 327–335
34. Johnsson, K., Froland, W. A., and Schultz, P. G. (1997) Overexpression, purification, and characterization of the catalase-peroxidase KatG from *Mycobacterium tuberculosis*. *J. Biol. Chem.* **272,** 2834–2840
35. Timmins, G. S., Master, S., Rusnak, F., and Deretic, V. (2004) Nitric oxide generated from isoniazid activation by KatG: Source of nitric oxide and activity against *Mycobacterium tuberculosis*. *Antimicrob. Agents Chemother.* **48,** 3006–3009
36. Zahrt, T. C., Song, J., Siple, J., and Deretic, V. (2001) Mycobacterial FurA is a negative regulator of catalase-peroxidase gene katG. *Mol. Microbiol.* **39,** 1174–1185
37. Pettijohn, D. E. (1988) Histone-like proteins and bacterial chromosome structure. *J. Biol. Chem.* **263,** 12793–12796
38. Heym, B., Zhang, Y., Poulet, S., Young, D., and Cole, S. T. (1993) Characterization of the katG gene encoding a catalase-peroxidase required for the isoniazid susceptibility of *Mycobacterium tuberculosis*. *J. Bacteriol.* **175,** 4255–4259
39. Rouse, D. A., DeVito, J. A., Li, Z., Byer, H., and Morris, S. L. (1996) Site-directed mutagenesis of the katG gene of *Mycobacterium tuberculosis*: Effects on catalase-peroxidase activities and isoniazid resistance. *Mol. Microbiol.* **22,** 583–592
40. Sherman, D. R., Mdluli, K., Hickey, M. J., Arain, T. M., Morris, S. L., Barry, C. E., 3rd, and Stover, C. K. (1996) Compensatory ahpC gene expression in isoniazid-resistant *Mycobacterium tuberculosis*. *Science* **272,** 1641–1643
41. Takatsuka, M., Osada-Oka, M., Satoh, E. F., Kitadokoro, K., Nishiuchi, Y., Niki, M., Inoue, M., Iwai, K., Arakawa, T., Shimoji, Y., Ogura, H., Kobayashi, K., Rambukkana, A., and Matsumoto, S. (2011) A histone-like protein of mycobacteria possesses ferritin superfamily protein-like activity and protects against DNA damage by Fenton reaction. *PLoS One* **6,** e20985
42. Yeruva, V. C., Duggirala, S., Lakshmi, V., Kolarich, D., Altmann, F., and Sritharan, M. (2006) Identification and characterization of a major cell wall-associated iron-regulated envelope protein (Irep-28) in *Mycobacterium tuberculosis*. *Clin. Vaccine Immunol.* **13,** 1137–1142
43. Handwerger, S., and Tomasz, A. (1985) Antibiotic tolerance among clinical isolates of bacteria. *Rev. Infect. Dis.* **7,** 368–386
44. Smith, A. L., Fiel, S. B., Mayer-Hamblett, N., Ramsey, B., and Burns, J. L. (2003) Susceptibility testing of *Pseudomonas aeruginosa* isolates and clinical response to parenteral antibiotic administration: Lack of association in cystic fibrosis. *Chest* **123,** 1495–1502
45. Horne, D., and Tomasz, A. (1981) pH-dependent penicillin tolerance of group B streptococci. *Antimicrob. Agents Chemother.* **20,** 128–135

46. Kim, K. S., and Bayer, A. S. (1987) Significance of *in vitro* penicillin tolerance in experimental enterococcal endocarditis. *J. Antimicrob. Chemother.* **19,** 475–485
47. Goodell, E. W., Fazio, M., and Tomasz, A. (1978) Effect of benzylpenicillin on the synthesis and structure of the cell envelope of *Neisseria gonorrhoeae*. *Antimicrob. Agents Chemother.* **13,** 514–526
48. Tuomanen, E. (1986) Phenotypic tolerance: The search for β-lactam antibiotics that kill nongrowing bacteria. *Rev. Infect. Dis.* **8,** S279–291
49. Bradley, M. D., Beach, M. B., de Koning, A. P., Pratt, T. S., and Osuna, R. (2007) Effects of Fis on *Escherichia coli* gene expression during different growth stages. *Microbiology* **153,** 2922–2940
50. Ali Azam, T., Iwata, A., Nishimura, A., Ueda, S., and Ishihama, A. (1999) Growth phase-dependent variation in protein composition of the *Escherichia coli* nucleoid. *J. Bacteriol.* **181,** 6361–6370

Dominant Incidence of Multidrug and Extensively Drug-Resistant Specific *Mycobacterium tuberculosis* Clones in Osaka Prefecture, Japan

Aki Tamaru[1,2*], Chie Nakajima[3], Takayuki Wada[4], Yajun Wang[2], Manabu Inoue[2], Ryuji Kawahara[1], Ryoji Maekura[5], Yuriko Ozeki[6], Hisashi Ogura[7], Kazuo Kobayashi[8], Yasuhiko Suzuki[3,9], Sohkichi Matsumoto[2]

1 Department of Infectious Diseases, Osaka Prefectural Institute of Public Health, Osaka, Osaka, Japan, **2** Department of Bacteriology, Osaka City University Graduate School of Medicine, Osaka, Japan, **3** Division of Global Epidemiology, Hokkaido University Research Center for Zoonosis Control, Sapporo, Hokkaido, Japan, **4** Department of Microbiology, Osaka City Institute of Public Health and Environmental Sciences, Osaka, Japan, **5** Department of Internal Medicine, National Hospital Organization National Toneyama Hospital, Toyonaka, Osaka, Japan, **6** Department of Food and Nutrition, Sonoda Women's University, Amagasaki, Hyogo, Japan, **7** Department of Virology, Osaka City University Graduate School of Medicine, Osaka, Japan, **8** Departement of Immunology, National Institute of Infectious Diseases, Shinjyuku-ku, Tokyo, Japan, **9** Japan Science and Technology Agency/Japan International Cooperation Agency-Science and Technology Research Partnership for Sustainable Development, Chiyoda-ku, Tokyo, Japan

Abstract

Infection and transmission of multidrug-resistant *Mycobacterium tuberculosis* (MDR-Mtb) and extensively drug-resistant *M. tuberculosis* (XDR-Mtb) is a serious health problem. We analyzed a total of 1,110 Mtb isolates in Osaka Prefecture and neighboring areas from April 2000 to March 2009. A total of 89 MDR-Mtb were identified, 36 (48.5%) of which were determined to be XDR-Mtb. Among the 89 MDR-Mtb isolates, 24 (27.0%) phylogenetically distributed into six clusters based on mycobacterial interspersed repetitive units-various number of tandem repeats (MIRU-VNTR) typing. Among these six clusters, the MIRU-VNTR patterns of four (OM-V02, OM-V03, OM-V04, and OM-V06) were only found for MDR-Mtb. Further analysis revealed that all isolates belonging to OM-V02 and OM-V03, and two isolates from OM-V04 were clonal. Importantly such genotypes were not observed for drug-sensitive isolates. These suggest that few but transmissible clones can transmit after acquiring multidrug resistance and colonize even in a country with a developed, well-organized healthcare system.

Citation: Tamaru A, Nakajima C, Wada T, Wang Y, Inoue M, et al. (2012) Dominant Incidence of Multidrug and Extensively Drug-Resistant Specific *Mycobacterium tuberculosis* Clones in Osaka Prefecture, Japan. PLoS ONE 7(8): e42505. doi:10.1371/journal.pone.0042505

Editor: Jean Louis Herrmann, Hopital Raymond Poincare - Universite Versailles St. Quentin, France

Received February 7, 2012; **Accepted** July 9, 2012; **Published** August 31, 2012

Funding: This work was supported by a grant from the Ministry of Health, Labour and Welfare (Research on Emerging and Reemerging Infectious Diseases, Health Sciences Research Grants) to AT, TW, KK and SM, and a grant from Osaka City University to SM, RM and AT, by a grant from United States-Japan Cooperative Medical Science Programs, by the Global Center of Excellence Program, "Establishment of International Collaboration Centers for Zoonosis Control", Ministry of Education, Culture, Sports, Science and Technology (MEXT), Japan, by Grants-in-Aid for the Program of Founding Research Center for Emerging and Re-emerging Infectious Diseases from MEXT to YS as well as by Grants-in-Aid for Scientific Research from Japan Society for the Promotion of Science to YS and CN. The funders had no role in study design, data collection and analysis, decision to publish, or preparation of the manuscript.

Competing Interests: The authors have declared that no competing interests exist.

* E-mail: tamaru@iph.pref.osaka.jp

Introduction

The control of tuberculosis (TB) has become increasingly more urgent because of the emergence of multidrug-resistant tuberculosis (MDR-TB) and extensively drug-resistant tuberculosis (XDR-TB). These two forms of TB are difficult to manage and treat, and known for producing high morbidity and mortality [1,2]. Multidrug-resistant *Mycobacterium tuberculosis* (MDR-Mtb) is resistant to at least both isoniazid (INH) and rifampin (RFP), while extensively drug-resistant *M. tuberculosis* (XDR-Mtb) is resistant to both INH and RFP, in addition to any of the second-line injectable drugs (capreomycin, kanamycin [KM] or amikacin) and fluoroquinolone [3,4]. In principle, these resistant *M. tuberculosis* (Mtb) strains are thought to arise through the selection of mutated strains in response to inadequate chemotherapy [1,2,5,6]. It is generally believed that transmission frequency of MDR/XDR-Mtb is lower comparing to drug-susceptible strains, however, exogenous infection with MDR/XDR-Mtb was reported, especially in countries with high human immunodeficiency virus (HIV) infection rates [6–8].

Several studies that genotyped MDR-Mtb isolates have shown that some are genetically related, forming phylogenetic clusters with identical genotypes [9–12]. Most of these reports showed that MDR-Mtb genetic clusters consist of isolates that belong to the Beijing genotype [7,10,12], suggesting a high tendency to become MDR-Mtb Beijing strains. Beijing strains are endemically predominant in East Asia [13] and are epidemically spreading in isolated regions such as Cuba, Eastern Europe, sub-Saharan Africa, and Vietnam [14]. Overall, Beijing strains of Mtb represent approximately 10% of MDR-Mtb isolates worldwide [14].

In 2009, Japan had intermediate TB incidence (19.0/100,000) [15] and a low HIV infection rate (new HIV infections, 0.8/100,000) (calculated from data in [16]). The prevalence of new MDR-TB cases in Japan was 0.7% and new XDR-TB cases was 0.2% [17]. Using this statistical ratio, it is estimated that approximately 170 new MDR-TB cases including approximately

50 XDR-TB cases occur every year. Moreover, greater than 70% of all Mtb isolated in Japan were of the Beijing genotype [18].

Osaka Prefecture has historically had the highest endemic rate of TB in Japan since 1991. The rate of TB incidence in Osaka in 2009 was determined to be 31.5/100,000 (16), while maintaining a low HIV infection rate (1.9/100,000) (calculated from data in [16]). Osaka Prefecture is located in central Japan and has an area of 1,989 km^2. It is a highly industrialized area including Osaka, the third most populous city in Japan, and over 8 million people have lived in Osaka Prefecture since 1973. In Osaka, both MDR-TB and XDR-TB cases have been reported, but little is known about the transmission of MDR/XDR-Mtb and the prevalence of Beijing lineage genotypes among MDR-Mtb isolates.

In the present study, we characterized a total of 1,110 Mtb isolates obtained from TB patients in Osaka prefecture and a neighboring area utilizing mycobacterial interspersed repetitive units-various number of tandem repeats (MIRU-VNTR) typing to investigate transmission of MDR-TB. Our data revealed that MDR/XDR-Mtb clones displayed genotypes that are not typically seen in drug-susceptible isolates and these strains are colonizing and spreading in Osaka Prefecture and its neighboring area.

Materials and Methods

Mtb Isolates

We analyzed 89 MDR-Mtb and 1021 non MDR-Mtb isolates collected in Osaka Prefectural Institute of public health. Eighty-nine MDR-Mtb isolates, which were delivered from three hospitals having tuberculosis ward in Osaka prefecture, were isolated from MDR-TB patients in Osaka Prefecture (except Osaka city and southeast area of Osaka prefecture) and neighboring local governments from April 2000 to March 2009. Of 1021 non MDR-Mtb isolates of which genetic diversity and/or genotypes were compared with those of MDR-Mtb, 471 isolates were sent to the institute for routine examinations (identifications of *Mtb*, drug susceptibility, and/or determination of the source of TB outbreaks) by Osaka prefectural health care centers from April 2000 to March 2007 and by neighboring local governments from April 2000 to March 2009. The remaining 550 were isolates from newly diagnosed TB patients in Osaka prefecture (except Osaka city and southeast area of Osaka prefecture) and sent to the institute for population-based molecular epidemiology of TB (population-based non MDR-Mtb). All Mtb isolates were confirmed whether they were MDR-Mtb or not in the laboratories of the hospitals, commercial laboratories, or Osaka Prefectural institute of public health. Although we could not fully obtain patient data including age, sex, residence area, year of case reported, and history of TB, duplication of patients of the isolates were avoided by the unified patients' identification numbers and the names of the patients.

Drug Susceptibility Test

To determine the ratio of XDR-Mtb for MDR-Mtb, we performed drug susceptibility tests of MDR-Mtb. When MDR-Mtb isolates were grown on Ogawa medium, 15 of the 89 isolates provided failed to grow on this medium because they perished. Therefore, for the remaining 74, minimum inhibitory concentrations (MICs) for INH, RFP, KM, streptomycin (SM), ethambutol (EB), and the fluoroquinolones, levofloxacin (LVFX), spafloxacin (SPFX), and ciprofloxacin (CPFX) were determined using the micro-dilution test BrothMIC MTB I (Kyokuto, Tokyo). Mtb isolates resistant to INH, RFP, KM and at least one fluoroquinolone were defined as XDR-Mtb.

DNA Extraction and Genotyping

Chromosomal DNA was extracted by combining chloroform extraction and mechanical disruption [19] from cultures grown on Ogawa medium or MGIT liquid medium for all 89 isolates. DNA was extracted from all 1110 isolates and genotyped using the MIRU-VNTR type testing [18,20] for 26 loci to identify transmission routes. Single-locus variants involving QUB4120, QUB11a, QUB11b, and QUB26 were regarded as identical in this study. All 89 MDR-Mtb isolates and 550 population-based non MDR-Mtb were examined by PCR to determine the frequency of the Beijing lineage [21]. Isolates determined as genetically related to the Beijing lineage were further classified into ancient and modern sub-lineages by PCR [22,23].

Sequence Analysis

MDR-Mtb isolates showing identical genetic patterns were analyzed by their SNPs for *katG*, *inhA*, *rpoB*, *rrs*, and *gyrA*. PCR products were amplified using the following primers: *katG*-Fw, CGCAGCGAGAGGTCAGTGGCCAG; *katG*-Rv, ATGGC-CATGAACGACGTCGAAAC; *inhA*-Fw, TCACACCGA-CAAACGTCACGAGC; *inhA*-Rv, AGCCAGCCGCTGTGC-GATCGCCA; *rpoB*-Fw, CAGGACGTGGAGGCGATCAC; *rpoB*-Rv, GAGCCGATCAGACCGATGTTGG; *rrs*-Fw, TCAC-CATCGACGAAGCTCCG; *rrs*-Rv, CTA-GACGCGTCCTGTGCATG; *gyrA*-Fw, AGCGCAGCTA-CATCGACTATGCG; and *gyrA*-Rv, CTTCGGTGTACCTCATCGCCGCC. All amplified products were purified and sequenced using the Big Dye Terminator Cycle Sequencing Kit (Applied Biosystems Inc., Japan) on a ABI Prism 3100 Genetic Analyzer (Applied Biosystems Inc.).

Results

Identification of MDR/XDR-Mtb and Drug Sensitivity Patterns

The drug susceptibility patterns of 74 MDR-Mtb isolates were identified to investigate the prevalence of XDR-Mtb among MDR-Mtb isolates (Table 1) and 36 (48.6%) were determined to be XDR-Mtb. Of these 36 XDR-Mtb, 25 (33.8%) were determined to be resistant to all eight drugs tested in this study. Of the 38 MDR-Mtb isolates, eight were resistant only to INH and RFP (10.8%), while the remaining 30 were resistant to INH, RFP, and either one or more second-line injectable drugs or one or more fluoroquinolone.

Comparison of the Genetic Diversity of MDR-Mtb and Non MDR-Mtb

To bring out the genetic aspects of MDR-Mtb, we compared the cluster formation resulting from MIRU-VNTR genotyping and the frequency of Beijing lineage with those of population-based non MDR-Mtb (Table2). Among 89 MDR-Mtb isolates, 24 (27.0%) isolates were classified into six identical clusters. In population-based non MDR-Mtb, sixty-five identical clusters were formed from 216 (39.3%) isolates. The ratio of cluster-forming isolates in MDR-Mtb was significantly lower than it in population-based non MDR-Mtb.

The frequency of the Beijing Lineage was 88.8% in MDR-Mtb and 77.3% in population-based non MDR-Mtb, showing significantly higher frequency of the Beijing Lineage in MDR-Mtb isolates. The Beijing lineage can be divided into ancient and modern sub-lineage by the insertion of IS*6110* into the NTF region of the genome [22]. About the ratio of ancient sub-lineage and modern, the significant difference was not seen in MDR-Mtb

Table 1. Drug resistance patterns of 74 MDR-TB isolates.

MDR or XDR	Total number of isolates (%)*	Drug resistance pattern								Number of isolates (%)*
XDR	36 (48.6)	INH	RFP	KM	SM	EB	LVFX	CPFX	SPFX	25 (33.8)
		INH	RFP	KM		EB	LVFX	CPFX	SPFX	8 (10.8)
		INH	RFP	KM			LVFX	CPFX	SPFX	1 (1.4)
		INH	RFP	KM			LVFX	CPFX		1 (1.4)
		INH	RFP	KM	SM		LVFX	CPFX	SPFX	1 (1.4)
MDR	38 (51.4)	INH	RFP		SM	EB	LVFX	CPFX	SPFX	4 (5.4)
		INH	RFP			EB	LVFX	CPFX	SPFX	4 (5.4)
		INH	RFP		SM		LVFX	CPFX	SPFX	1 (1.4)
		INH	RFP		SM			CPFX	SPFX	1 (1.4)
		INH	RFP		SM	EB		CPFX		1 (1.4)
		INH	RFP	KM	SM	EB				6 (8.2)
		INH	RFP		SM	EB				3 (4.1)
		INH	RFP			EB				5 (6.8)
		INH	RFP		SM					4 (5.4)
		INH	RFP	KM						1 (1.4)
		INH	RFP							8 (10.8)

*Percentage of MDR-TB isolates determined drug sensitivity.

doi:10.1371/journal.pone.0042505.t001

isolates and population-based non MDR-Mtb (75.9% and 77.2%, respectively).

Comparison of MIRU-VNTR Patterns between MDR-andnon-MDR-Mtb Isolates

The MIRU-VNTR patterns of the 6 identical clusters constructed from MDR-Mtb isolates OM-V02, OM-V03, OM-V04, OM-V06, OM-V12, and OM-V32 were shown in Table 3. To verify these MIRU-VNTR pattern were specific to MDR-Mtb isolates or not, we genotyped not only population-based non MDR-Mtb isolates but also other 471 non MDR-Mtb isolates (total 1021 non MDR-Mtb isolates were genotyped) and all MDR-Mtb clusters and non-MDR-Mtb clusters with incidence rates of more than 1.0% per total isolates are presented in Table 3. Importantly four clusters, OM-V02, OM-V03, OM-V04, and OM-V06, consisted of only MDR-Mtb isolates and none of the 1,021 non-MDR-Mtb isolates. These four clusters together were designated as a MDR-Mtb-specific cluster (MDR-Mtb SC). In particular, the incidence rate of OM-V02 (1.1% of 1,110 isolates) was the highest among the MDR-Mtb SC and equal to that of OM-V801, the sixth largest non-MDR-Mtb cluster.

In contrast, two of the six MDR-Mtb clusters, OM-V12 and OM-V32, had the MIRU-VNTR patterns that were also found in non-MDR-Mtb isolates. The other 65 MDR-Mtb isolates formed 10 clusters (OM-V29, OM-V05, OM-V031, OM-V091, OM-V021, OM-V070, OM-V067, OM-V08, OM-V068, and OM-V087) with one or multiple non-MDR-Mtb isolates. The clusters were designated as a mixed cluster (Mix C) type, of which MIRU-VNTR pattern were observed in both MDR and non-MDR Mtb. The remaining 55 MDR-Mtb showed unique MIRU-VNTR patterns.

Different incidence ratios of MDR/non-MDR-Mtb were observed among clusters. For example, OM-V29, which was the largest cluster, consisted of only one MDR-Mtb and 30 non-MDR-Mtb isolates, while two of nine isolates were MDR-Mtb in OM-V12 (the eighth largest cluster) and two of 13 were MDR-Mtb in OM-V32 (the third largest cluster).

Table 2. Comparison of the genetical diversity of MDR-Mtb and non MDR-Mtb.

	The number of clusters	The number of isolates		
		included in any clusters	belonging to Beijing Lineage	belonging to ancient sublineage
MDR-Mtb	6	24	79	60
		27.0%	88.8%	75.9%**
non MDR-Mtb	65	216*	425*	328
		39.3%	77.3%	77.2%**

*significant difference ($P<0.05$, Fisher's exact test).

**percentage for Beijing isolates.

doi:10.1371/journal.pone.0042505.t002

Table 3. MIRU-VNTR profiles of phylogenetic clusters.

Cluster type*	Cluster No.	Number of alleles in the MIRU-VNTR loci†	number of isolates in cluster			Beijing sublineage
			MDR	non MDR	(%)‡	
MDR-TB	OM-V02	2 1 3 8 7 3 5 2 4 4 4 3 4 3 4 3 5 2 4 4 7 4 9 7 8 10	11	0	(1.1)	ancient
	OM-V03	2 3 3 5 7 3 5 3 3 4 4 3a 2 3 4 2 4 3 3 2 10 4 25 6 8 4	4	0	(0.4)	ancient
	OM-V04	3 3 3 5 7 3 5 3 3 2 4 3 4 3 2 3 4 3 3 4 5 4 8 1 7 9	3	0	(0.3)	ancient
	OM-V06	2 3 3 5 7 3 5 3 3 3 4 3 4 4 3 3 3 3 3 4 7 4 5 5 8 10	2	0	(0.2)	modern
Mix C	OM-V12	2 3 4 5 7 2 5 3 3 4 4 3 3 3 4 3 5 4 3 5 7 2 8 8 2 11	2	7	(0.8)	ancient
	OM-V32	2 3 3 5 7 3 5 3 3 4 4 3 4 4 4 3 3 3 3 4 7 4 8 8 8 9	2	11	(1.2)	modern
	OM-V29	2 3 3 5 7 3 5 3 3 4 4 3 4 4 4 3 3 3 3 4 7 4 5 5 8 8	1	30	(2.8)	modern
	OM-V05	2 3 3 5 7 3 5 3 3 4 4 3a 3 3 4 3 4 3 3 2 10 4 5 5 6 8	1	16	(1.5)	ancient
	OM-V031	2 3 4 5 7 3 5 3 3 4 4 3 3 3 4 3 5 4 3 5 7 2 8 7 2 9	1	6	(0.6)	ancient
	OM-V091	2 3 3 5 7 3 5 3 3 4 4 3 4 3 4 3 5 2 3 4 7 4 5 7 10 8	1	4	(0.5)	ancient
	OM-V021	2 3 3 5 4 3 5 3 3 4 4 3 4 4 4 3 3 3 3 4 7 4 8 6 8 10	1	4	(0.5)	modern
	OM-V070	1 5 1 5 1 3 3 2 2 3 4 3a 2 2 4 3 4 1 3 2 12 2 7 2 9 3	1	3	(0.4)	non Beijing
	OM-V067	2 3 3 5 7 1 5 3 1 4 4 3 4 3 4 3 3 3 3 4 7 4 8 9 8 10	1	3	(0.4)	modern
	OM-V08	2 3 3 5 7 3 4 3 3 4 4 3 4 0 2 3 4 3 3 4 1 6 8 3 8 10	1	2	(0.3)	ancient
	OM-V068	2 3 3 6 5 3 3 1 1 3 3 3 2 1 2 6 3 3 2 4 12 2 2 2 3 2	1	1	(0.2)	non Beijing
	OM-V087	2 1 3 5 7 3 5 3 3 4 4 3 4 3 4 3 5 2 4 4 7 4 7 6 8 11	1	1	(0.2)	ancient
non MDR	OM-V127	2 3 4 5 7 3 5 3 3 4 4 3 3 3 4 3 5 4 3 5 7 2 8 7 2 11	0	13	(1.2)	ancient
	OM-V228	2 3 3 5 7 3 5 3 3 4 4 3a 4 3 4 3 5 3 3 4 7 4 8 7 8 5	0	13	(1.2)	ancient
	OM-V801	2 3 3 5 5 3 3 2 1 2 4 3a 2 1 2 3 3 2 2 4 8 4 2 2 4 2	0	11	(1.1)	ancient

*MDR: clusters consisted of only MDR-TB isolates, Mix C: clusters consisted of MDR-TB isolates and non MDR-TB isolates, non MDR: clusters consisted of only non-MDR-TB isolates for which the ratio of total non MDR-TB isolates is >1%.

†The order of MIRU-VNTR loci is as follows: 0580, 0960, 1644, 2531, 2996, 3007, 3192, 4348, 0802, 2165, 0577, 3239 (3a contains irregular-size alleles), 0424, 1955, 2401, 3690, 4156, 2074, 2372, 3155, 3336, 1895, 2163a, 2163b, 4052, 4120.

‡Percentage of all TB isolates.

doi:10.1371/journal.pone.0042505.t003

MIC Values and Mutation Patterns of MDR-Mtb SC

To further investigate whether isolates in each cluster in MDR-Mtb SC (OM-V02, OM-V03, OM-V04, and OM-V06) were identical clones, MICs and mutations in the resistance-associated genes were analyzed (Table 4). Although nine of these isolates (Nos. 010, 019, 030, 063, 073, 082, 095, and 004) belonging to OM-V02 were XDR-Mtb and the remaining two (051, 052) were MDR-Mtb, the MICs of these isolates revealed slight variations and all isolates possessed D516V in *rpoB*, S315T in *katG*, and a nucleotide substitution in *rrs* (adenine to guanine at position 1400 in the gene). Nos. 19 and 95 had additional mutations in *katG* and *rpoB*, respectively. Regarding isolates belonging to the OM-V03 cluster, of which MICs and mutations were similar for all isolates, only isolate No. 029 showed a higher MIC value to INH and an additional mutation in *inhA*. Isolate Nos. 002 and 020 in cluster OM-V04 shared the same MIC and mutation patterns. Taken together, these data suggest that OM-V02, OM-V03, and OM-V04 are three clonal strains.

We described characteristics of the cases with OM-V02, OM-V03, and OM-V04 in Table 5. About OM-V02, the age distribution of patients was wide and seven patients were younger than 60 years old. The earliest patients (Nos 019 and 073) were reported in 2002 and the last one (No. 063) was reported in 2008. In 11 patients, seven patients (005, 019, 050, 051, 082, 095, and 004) were newly diagnosed as MDR-TB. As to OM-V03, the age distribution of patients was the age of between 30 and 89, the period when patients reported was from 2000 to 2008, and two of four patients were newly diagnosed. Both patients with OM-V04 were newly diagnosed, one was reported in her 30's in 2002 and the other was reported in her 60's in 2003.

Discussion

To understand the transmission dynamics of MDR/XDR-Mtb in Osaka Prefecture and its neighboring region, an area with the highest TB endemicity in Japan, molecular epidemiological analyses of 89 MDR/XDR-Mtb was performed. Overall, our study demonstrated the following features of Mtb found in Osaka Prefecture and its neighboring regions: 1) a high XDR-Mtb to MDR-Mtb ratio (48.5%); 2) a high ratio (88.8%) of Beijing lineage genotypes among MDR-Mtb; 3) the spread of MDR/XDR-Mtb isolates that share distinct MIRU-VNTR patterns.

Our data revealed a high XDR-Mtb to MDR-Mtb ratio (48.5%) in the studied area. The XDR/MDR ratio in Japan, 31.5% [17] is higher than that of other countries [2,24]. One of the causes for this high ratio seems to be the presence of the MDR-Mtb SC. Two of the MDR-Mtb SC consisted of only XDR-Mtb isolates and one contained nine XDR-Mtb (Table 4). By excluding XDR-Mtb isolates from the MDR-Mtb SC, the XDR/MDR ratio in this study was determined to be 40.0%, which is still significantly higher than the national ratio. From the available information, we cannot specify what factors result in the increase in XDR/MDR ratio in Osaka. In Osaka Prefecture and Japan, the prevalence of TB patients co-infected with HIV is low,